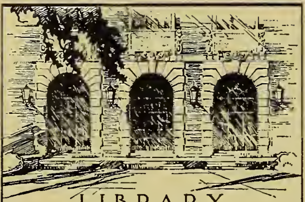

LIBRARY
OF THE
UNIVERSITY
OF ILLINOIS
621.365
Il655te
no. 50-57
cop. 2

~~ENGINEERING~~

Digitized by the Internet Archive
in 2013

http://archive.org/details/inputimpedanceso56tang

Antenna Laboratory

Technical Report No. 56

INPUT IMPEDANCES OF SOME CURVED WIRE ANTENNAS

by

C. H. Tang

Contract AF33(657)-8460

Project No. 6278, Task No. 40572

June 1962

Sponsored by:

AERONAUTICAL SYSTEMS DIVISION

Electrical Engineering Research Laboratory
Engineering Experiment Station
University of Illinois
Urbana, Illinois

Antenna Laboratory

Technical Report No. 56

INPUT IMPEDANCES OF SOME CURVED WIRE ANTENNAS

by

C. H. Tang

Contract AF33(657)-8460

Project No. 6278, Task No. 40572

June 1962

Sponsored by:

AERONAUTICAL SYSTEMS DIVISION

Electrical Engineering Research Laboratory
Engineering Experiment Station
University of Illinois
Urbana, Illinois

21.365
l 655t
no.56
cop.2

ACKNOWLEDGEMENT

The author wishes to express his deep appreciation of the guidance of Professor G. A. Deschamps whose advice and suggestions were always illuminating. Many helpful discussions with members of the antenna laboratory are acknowledged. The computer program used in this work was done by Mr. V H. Gonzalez. It is a pleasure to acknowledge the financial support of Wright Air Development Division of the United States Air Force.

ABSTRACT

The problem of the input impedance of curved wire antennas is formulated in terms of an integral equation. A stationary formula is used in evaluating the input impedances of arc antennas and helical antennas of which the cylindrical antenna is a special case. The computational results are presented in graphical form. The impedance characteristics of these curved antennas are discussed.

CONTENTS

Page

1. Introduction 1

2. Integral Equation Formulation for Wire Antennas 4

2.1 Integro-Differential Equation for Thin Wire Antennas 4
2.2 Linearization 9
2.3 Transformation of the Integro-Differential Equation 11
2.4 The Singular Integral Equation and the Approximate Kernel Function 13
2.5 Structures Which Give Closed Cycle Type Kernels 17

3. Variational Formulation of the Input Impedance of Wire Antennas 20

3.1 Derivation of the Variation Function 20
3.2 The First Order Solution and the Assumed Current Distribution 23
3.3 Higher Order Solutions 25
3.4 First Order Solution for Arc Antennas and Helical Antennas 28

4. Computational Results and Discussions 35

4.1 Computational Method 35
4.2 The Input Impedances of Cylindrical Antennas 36
4.3 The Input Impedance of Arc Antennas 44
4.4 Electromagnetic Resonance of Thin Wire Conductors 54
4.5 The Input Impedances of Helical Antennas 59
4.6 Equivalent Helical Antennas 72

5. Summary of the Results and Conclusions 75

Bibliography 78

Appendix A 79

Appendix B 82

Appendix C 89

ILLUSTRATIONS

Figure Number		Page
1	An Idealized Antenna Structure	5
2	Bent Cylindrical Coordinate System	6
3	A Helical Antenna	8
4	An Arc Antenna	9
5	A Center Driven Idealized Cylindrical Antenna	15
6	The Input Impedances of Cylindrical Antennas ($k\ell$ = 1.5 to 3.7)	40
7	The Input Impedances of Cylindrical Antennas ($k\ell$ = 4.7 to 6.9)	41
8	The Input Impedances of Cylindrical Antennas ($k\ell$ = 7.9 to 9.9)	42
9	The Input Impedances of Arc Antennas	45
10	Resonant Resistances of Arc Antennas	47
11	Antiresonant Resistances of Arc Antennas	48
12	Resonant Lengths and Antiresonant Lengths for Arc Antennas	49
13	Shortenings of Resonant Length and Antiresonant Length of Arc Antennas	50
14	The Ratio of Resonant Wavelength to Arc Length as a Function of C_1 -- Comparison Between Englund's Measured Results and That Obtained From the Impedance Graphs.	51
15	Resistive Part of the Input Impedance Along Equi-$k\ell$ Contours	53
16	The Input Impedances of Helical Antennas $C_1 = .5$	60
17	The Input Impedances of Helical Antennas $C_1 = 0.75$	61
18	The Input Impedances of Helical Antennas $C_1 = 1$	62
19	Resonant Resistance as a Function of Pitch in Wavelength	63

ILLUSTRATIONS (Cont'd)

Figure Number		Page
20	Antiresonant Resistance as a Function of Pitch in Wavelength	64
21a	The Input Impedances of Helical Antennas $C_2 = 0.25$	65
21b	The Input Impedances of Helical Antennas $C_2 = 0.25$	66
22a	The Input Impedances of Helical Antennas $C_2 = 0.5$	67
22b	The Input Impedances of Helical Antennas $C_2 = 0.5$	68
23	Resonant Resistance as a Function of Circumference in Wavelength	70
24	Antiresonant Resistance as a Function of Circumference in Wavelength	71
25	Equal Resonant Resistance Contours	73
26	Equal Antiresonant Resistance Contours	74

1. INTRODUCTION

It is of practical importance to know the characteristics of the input impedance of an antenna, as a function of the frequency of the source and the geometry of the antenna structure. As far as wire antennas are concerned, the input impedance of cylindrical antennas has been investigated to a great extent by many authors[1,2,3,4]; but practically no theoretical results have been obtained in the case of curved wires. The problem to be considered in this report is that of evaluating the input impedance for some particular curve wires.

The theoretical model used in formulating the problem is the idealized wire antenna with a δ-source excitation, which is usually called a slice generator. This idealization avoids the problem of the actual transition between the transmission line and the radiating part of the antenna. With proper end zone correction, the input impedance computed from the theoretical model becomes the terminal impedance of the transmission line. In this report, only the idealized antenna problem will be considered.

The integral equation formulation for the electromagnetic problem is an important technique in antenna analysis, especially for cylindrical antennas. It was first used by Pocklington[5] and later developed by Hallén[2]. The method has the advantage of generality and is conceptually simple, although rigorous solutions are in general difficult to obtain. A large number of papers have been written on its application to cylindrical antennas using various means of approximation, much less attention was paid to the discussion of curved wire structures[6,7].

With the aid of the integral equation formulation, it can be shown that the input impedance of an antenna can be expressed in such a way that it is

stationary with respect to the current distribution in the antenna. It is recognized that the integral equation for the current distribution serves as an Euler equation of the variational problem of the input impedance. The well known Hallen iterative solution to the integral equation has been shown to give a good result for thin antennas, for which the asymptotic solution of the current distribution is known to be sinusoidal. The asymptotic solution, when applicable, can be used in the variational expression for the input impedance. Storer[8] and Tai[9] have calculated the input impedance of thin cylindrical antennas by such a method. Their results agree well with those obtained by the iteration method. We shall extend these solutions to some curved wire antennas.

Those curved wire antennas which we shall discuss are (1) arc antennas -- the antenna arms are bent into the shape of circular arcs with a given radius. (2) Helical antennas -- the antenna arms are sections of a helix with a given radius and pitch. Cylindrical antennas are special cases of these two classes. The common property of being invariant under a one dimensional Abelian group of congruent transformations sets these structures apart. This particular symmetry implies that the kernel of the linearized integral equation has a special form.

$$K(s,s') = K(|s - s'|)$$

This is known as a closed cycle type kernel. The above mentioned structures are the only ones which lead to such a kernel.

In this work, the computation of input impedances have been performed for both arc antennas and helical antennas. Results are shown in graphical forms. For arc antennas the input impedances are given for various radii

of the arc while those of helical antennas are shown as functions of the radius and the pitch of the helix. The computational results show the following general trend: in comparison with the cylindrical antenna, the curved wire antenna has a higher quality factor Q and radiates less with respect to the same input current. In many respects, a curved wire antenna behaves like a corresponding thinner cylindrical antenna. The input impedance graph for the arc antennas also exhibits the extreme phenomena observed by Englund in his measurements for the natural period of linear conductors[10].

Based on the computed input impedances of helical antennas the contour lines of equivalent helical antennas are given and they are closely described by the circles for the constant radius of the curvature of the helix.

2. INTEGRAL EQUATION FORMULATION FOR WIRE ANTENNAS

2.1 Integro-Differential Equation for Thin Wire Antennas

It is well known that in electromagnetic problems one can find the electric field strength $\vec{E}$ produced by current source $\vec{J}$ through the use of the vector potential function $\vec{A}$

$$j\omega\epsilon \vec{E} = [\mathrm{grad\,div} + k^2] \vec{A} \tag{1}$$

with

$$\vec{A}(x) = \frac{1}{4\pi} \int_v \vec{J}(x') \, G(x,x') \, dv \tag{2}$$

In Equation (1) k is the free space propagation constant. The integration in Equation (2) is performed over the source region v and G(x,x') is a Green's function of the vector wave equation

$$\nabla^2 \vec{A} + k^2 \vec{A} = -\vec{J} \tag{3}$$

with appropriate boundary conditions. However, in a general case it is not possible to find the Green's function for the region outside the antenna, with specified boundary conditions on the antenna surface, therefore we reduce the antenna problem to the problem of currents in free space and let

$$G(x,x') = \frac{e^{-jkr(x,x')}}{r(x,x')} \tag{4}$$

where r(x,x') is the linear distance between the source point x' and the observation point x.

Equations (1) and (2) are the basic relations for the antenna analysis. If the current distribution $\vec{J}$ was given, the field strength $\vec{E}$ could readily

be evaluated. If, on the other hand, the tangential electric field strength is specified on a close surface enclosing the antenna, then Equations (1) and (2) lead to an integro-differential equation for the current distribution on the antenna. For convenience, the surface is usually taken on the boundary of the antenna, and we shall discuss only antennas made of perfect conductors.

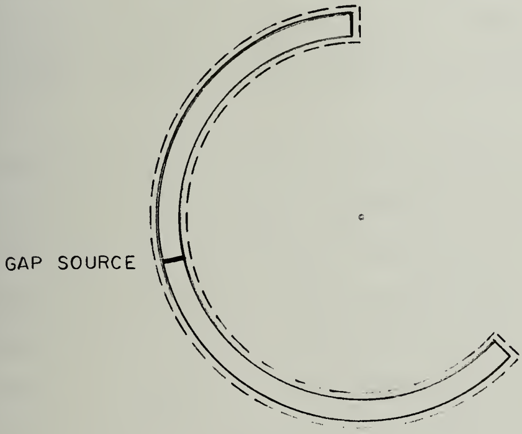

Figure 1. An idealized antenna structure

Since the tangential electric field vanishes on the antenna surface, the boundary value problem can be formulated in terms of an integro-differential equation with the relation

$$\vec{E}_t = - \vec{E}_t^{\,i} \tag{5}$$

where

$\vec{E}_t$ is the tangent electric field deduced from Equation (1)

$\vec{E}_t^{\,i}$ is the given impressed field which is assumed to be a δ-function

The integro-differential equation so formulated will give a unique solution if the support for the current distribution is specified.

For a general antenna surface, the vector integro-differential relation leads to two coupled scaler integro-differential equations for two components of the current distribution. However, for thin antennas of unifrom cross-section, the current flow is mostly in the axial direction; therefore we have a single two-dimensional integro-differential equation, instead of two. For the thin wire antennas of circular cross sections, the integro-differential equation can be expressed with the aid of a bent cylindrical coordinate system.

Figure 2 describes a bent cylindrical coordinate system. $\vec{C}$ (s) is a given smooth curve, $\hat{s}$ is the unit tangential vector at s, $\hat{n}$ is the unit principal normal vector and $\hat{b}$ is the unit binomal vector. A point p in the $\hat{n}$-$\hat{b}$ plane is described by the polar coordinates (ρ, φ) and hence any point in the neighborhood of the curve can be described by (ρ, φ, s). This coordinate system is not ambiguous if ρ is small compared to the radius of curvature. The Euclidean distance between two points on the wire surface, $P(a,\varphi,s)$ and $P'(a,\varphi',s')$, is designated by $r(s,s',\varphi, \varphi')$.

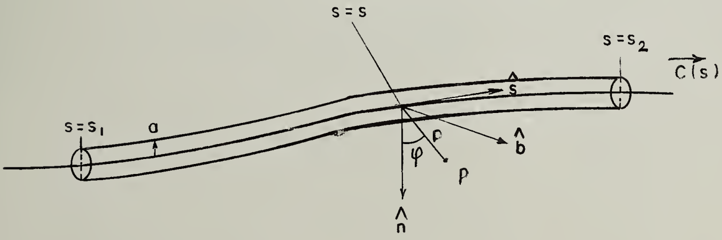

Figure 2. Bent cylindrical coordinate system

In the bent cylindrical coordinate system, the integro-differential equation for the thin wire antennas of circular cross sections can thus be written as

$$-j\omega\epsilon\, E_t^{\,i}(s,\varphi) = \frac{1}{4\pi}\int_{s_1}^{s_2}\int_{0}^{2\pi} K(s,s',\varphi,\varphi')\, J(s',\varphi')\, d\varphi'\, ds' \qquad (6)$$

where

$J(s',\varphi')$ is the current density at (a,φ',s') in the direction parallel to the axial tangent at s'

$E_t^{\,i}(s,\varphi)$ is the specified impressed field at (a,φ,s) in the direction parallel to axial tangent at s

and

$$K(s,s',\varphi,\varphi') = \left[-\frac{\partial^2}{\partial s\partial s'} + k^2(\hat{s}\cdot\hat{s}')\right]\frac{e^{-jkr(s,s',\varphi,\varphi')}}{r(s,s',\varphi,\varphi')} \qquad (7)$$

The expression for $r(s,s',\varphi,\varphi')$ is known when the geometric configuration of the antenna is given. For cylindrical antennas, we have

$$r = \left[(Z-Z')^2 + 4a^2\sin^2\left(\frac{\varphi-\varphi'}{2}\right)\right]^{1/2} \qquad (8)$$

where

$$Z = s$$

and

a is the radius of the wire

For helical antennas, we can write

$$r = \left\{ R_o^2 \left[2 - 2 \cos \frac{s-s'}{R_o} + \tan^2 \psi \left(\frac{s-s'}{R_o}\right)^2 \right] \right.$$

$$+ 2a^2 \left[1 + \sin \psi \sin (\varphi-\varphi') \sin \left(\frac{s-s'}{R_o}\right) - \cos \varphi \cos \varphi' \cos \left(\frac{s-s'}{R_o}\right)\right.$$

$$\left. -\sin\varphi \sin\varphi' \left(\sin^2 \psi \cos \frac{s-s'}{R_o} + \cos^2 \psi\right) \right] + 2aR_o\left[(\cos\varphi + \cos \varphi')\left(1-\cos\frac{s-s'}{R_o} \right)\right.$$

$$\left.\left. + \sin \psi (\sin\varphi - \sin\varphi')\left(\sin\frac{s-s'}{R_o} - \frac{s-s'}{R_o}\right) \right] \right\}^{1/2} \qquad (9)$$

where

ψ is the pitch angle

$\tan \psi = \frac{p}{2\pi R_o}$

and

R_o is the radius of the helix

p is the pitch of the helix

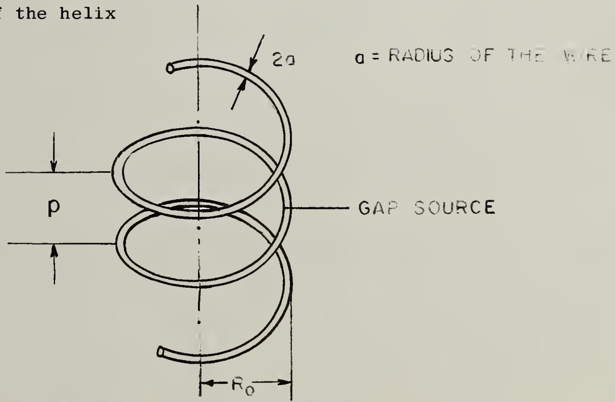

Figure 3. A helical antenna

For arc antennas, $\psi = 0$, and Equation (9) becomes

$$r = \left\{ [2R_o^{\;2} + 2aR_o (\cos \varphi + \cos \varphi')] (1 - \cos \frac{s-s'}{R_o}) + 2a^2 [1 - \cos (\frac{s-s'}{R_o}) \cos \varphi \cos \varphi' - \sin \varphi \sin \varphi'] \right\}^{1/2} \tag{10}$$

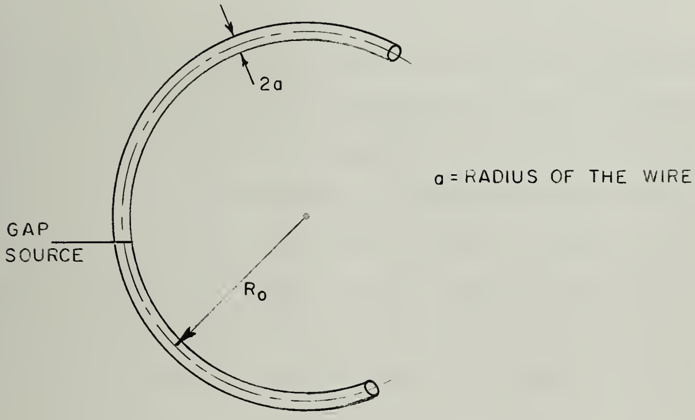

Figure 4. An Arc Antenna

2.2 Linearization

When the wire is thin, $ka \ll 1$, $|s_2 - s_1| \gg a$, the circumferential variation of the current is small and Equation (6) can be written as

$$-j\omega\epsilon\, E_t^{\;i}(s) = \frac{1}{4\pi}\int_{s_1}^{s_2} K_a(s,s')\, I(s')\, ds' \tag{6'}$$

where

$$I(s) = 2\pi J(s)$$

$$K_a(s,s') = \left(-\frac{\partial^2}{\partial s \partial s'} + k^2(\hat{s} \cdot \hat{s}')\right) G_a(s,s') \qquad (11)$$

and where

$$G_a(s, s') = \frac{1}{2\pi}\int_o^{2\pi} \frac{e^{-jkr(s,s',\varphi)}}{r(s,s',\varphi)} \, d\varphi \qquad (12)$$

which is an averaged Green's function. In Equation (12) we have interchanged the operator $\left(-\frac{\partial^2}{\partial s \partial s'} + k^2(\hat{s} \cdot \hat{s}')\right)$ and the integration operator. Generally this would cause inaccuracies due to the asymmetry of the curve wire. However, if the wire is small, the approximation is justified by the following arguments: (1) when $s - s'$ is large, the distance between two points on the wire surface can be taken to be the same as the two points on the axis of the wire, and (2) when $s - s'$ is small, the portion of the wire of interest is practically a circular cylinder in which case the above exchange of operators is valid.

In so doing, we have transformed the two dimensional equation into a one dimensional one. The boundary condition is satisfied only at a certain line on the wire surface, $\varphi = \varphi_o$; for convenience, we let $\varphi_o = 0$. This also involves approximations and can again be justified on the basis of the above mentioned arguments (1) and (2). This process of reducing a two-dimensional integral equation to a one-dimensional one is called linearization by Hallén.

The rigorous expression for $K_a(s,s')$ is generally very complicated, as indicated by the expression of $r(s,s',\varphi,\varphi')$ in Equations (9) and (10). Approximations are usually introduced at this stage to facilitate the

solution. We shall come back to this matter later, but we will first discuss the transformation of the integro-differential equation into an integral equation. It will be seen that the asymptotic solution for the potential and the current in a thin wire are both sinusoidal.

2.3 Transformation of the Integro-Differential Equation

To deduce the above result, the integro-differential equation of the wire antenna derived in Chapter 2.1 may be transformed into either a differential equation or an integral equation. Pocklington used the first approach to show that the asymptotic current distribution in a thin wire is sinusoidal while Hallén's endeavor was to transform the integro-differential equation into an integral equation of the second kind and then to obtain the solution by an iterative procedure. These are well known classical results. We shall reproduce the transformation procedure to include the application to the curved wire.

In general, we define the function

$$A(s) = \frac{1}{4\pi}\int_{s_1}^{s_2} I(s')\, N(s,s')\, G_a(s,s')\, ds' \tag{13}$$

where

$$N(s,s') = -\left[\frac{\partial r}{\partial s'}\right]\left[\frac{\partial r}{\partial s}\right]^{-1} \tag{14}$$

Then Equation (6) becomes

$$\left(\frac{d^2}{ds^2} + k^2\right) A(s) = -j\omega\epsilon\, E_t^i(s) - c(s) \tag{15}$$

where

$$c(s) = \int_{s_1}^{s_2} M(s,s')\ I(s')\ ds' \qquad (16)$$

and

$$M(s,s') = k^2 \left[(\hat{s} \cdot \hat{s}') - N(s,s') \right] G_a(s,s') - \frac{\partial}{\partial s} \left[\frac{\partial N}{\partial s} G_a(s,s') \right] \qquad (17)$$

c(s) in Equation (15) can be considered as a secondary source representing the effect of the curvature. It is seen that for cylindrical antennas

$$N = 1$$

$$(\hat{z} \cdot \hat{z}') = 1$$

Therefore M = 0 and there is no curvature effect. The function in Equation (13) becomes the axial component of the vector potential function which satisfies the one dimensional wave equation

$$\left(\frac{d^2}{dz^2} + k^2 \right) A(z) = -j\omega\epsilon\ E_t^{\ i}(z) \qquad (18)$$

Therefore for center-fed cylindrical antennas, A(z) can be expressed either in terms of standing waves

$$A(z) = C_1 \cos kz + C_2 \sin k|z| \qquad (19)$$

or in terms of traveling waves

$$A(z) = D_1\ e^{-jkz} + D_2 e^{jkz} + D_3 e^{-jk|z|} \qquad (20)$$

The constants C_1 and C_2 (or D_1, D_2 and D_3) are determined by the source condition and the boundary condition of the current I(z). If the source condition is given as

$$E_t^{\,i}(z) = V\,\delta(z) \tag{21}$$

then

$$C_2 = -j\,\frac{V}{2\zeta} \qquad \text{or} \qquad D_3 = \frac{V}{2\zeta} \tag{22}$$

where ζ is the characteristic impedance of free space.

The integral equation for cylindrical antennas of length 2ℓ is thus

$$\frac{1}{4\pi}\int_{-\ell}^{\ell} I(z')\,G_a(z,z')\,dz' = c_1 \cos kz - j\,\frac{V}{2\zeta}\sin k(z) \tag{23}$$

for the standing wave type solution.

In case of curved wire antennas, we solve A(s) from Equation (15) which gives for symmetric antennas

$$A(s) = C_1 \cos ks - j\,\frac{V}{2\zeta}\sin ks + \frac{1}{k}\int_{o}^{s} \sin k(s-s')\,C(s')\,ds' \tag{24}$$

Equations (24) and (13) also give an integral equation for curved wire antennas.

2.4 The Singular Integral Equation and the Approximate Kernel Function

The integral equation for the antenna problem so formulated has a singularity in its kernel function; when the observation point is approaching the source point, the value of the kernel function increases indefinitely. It

can be shown that in the neighborhood of the singularity the kernel function behaves as[11]

$$G_a(s,s') \xrightarrow{s\to s'} \frac{1}{\pi a} \ln \frac{8a}{|s-s'|} - jk \qquad (25)$$

As far as the singularity is concerned, the kernel function for the curved wire and that for the cylindrical wire have the same asymptotic behavior, since any smoothly curved wires are locally straight.

The function in Equation (25) is square integrable, for

$$\int_0^{\ell}\int_0^{\ell} \ln^2 |s-s'| \, ds' \, ds < \infty \qquad 0 \leq s \leq \ell, \; 0 \leq s' \leq \ell$$

hence the kernel is of the Fredholm type. Fredholm's alternative theroem is therefore applicable. Either the inhomogeneous equation is solvable, or else the corresponding homogeneous equation has a non-trivial solution.

However, if the size of the wire becomes infinitesimally small, the singularity of the kernel function is of higher order than that in Equation (25).

$$G(s,s') \xrightarrow{s\to s'} \frac{1}{|s-s'|} \qquad (26)$$

The integral of this function does not exist even in Canchy's principal value sense. This fact is known in potential theory; the attraction of a line of mass upon one of its own points does not have a definite meaning, while for surface distributions and volume distributions the potential function together with its derivative exists inside the source region (see The Theory of the Potential by W. D. Mac Millan).

In the light of these considerations, one realizes that the problem should be formulated with the finite size model for which the solution is predicted by the Fredholm theorem.

It was indicated in Section 2.2 that the rigorous expression of the averaged function $G_a(s,s')$ is rather complicated, even for cylindrical wires[6]

$$G_a(z,z') = \frac{k}{\pi a} F\left(\frac{1}{2}\pi, h\right) - \frac{1-e^{-jk|z-z'|}}{|z-z'|} + O(k^2a^2) \tag{27}$$

where

$$h = 2a[(z-z')^2 + 4a^2]^{-1/2}$$

is the modulus of the elliptic integral F. Usually, the simplification is obtained by introducing an approximation to the averaged kernel function of the integral equation.

For cylindrical antennas, Hallén derived the linearized equation

$$\log \frac{4(\ell^2-z^2)}{a^2} + \int_{-\ell}^{+\ell} \frac{I(z')e^{-jk|z-z'|} - I(z)}{|z-z'|} dz' = 4\pi\left[C_1 \cos hz - j\frac{V}{2\zeta} \sin k|z|\right] \tag{28}$$

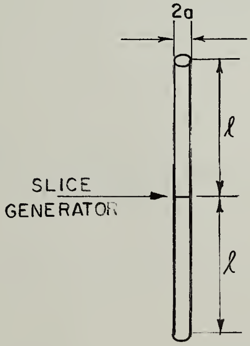

Figure 5. A center driven idealized cylindrical antenna

y splitting the kernel function into two terms; one depends on the size of he wire and has the static characteristic, while the other term is independent of the size.

$$\pi A(z) = I(z)\,\frac{1}{2\pi}\int_{-\ell}^{+\ell}\int_{0}^{2\pi}\frac{d\varphi'\,dz'}{\sqrt{(z-z')^2+4a^2\sin^2\frac{\varphi'}{2}}} + \int_{-\ell}^{+\ell}\frac{I(z')e^{-jk|z-z'|}-I(z)}{|z-z'|}\,dz' \qquad (29)$$

t is readily seen that the following approximation is good except very close o the end of the wire

$$\frac{1}{2\pi}\int_{0}^{2\pi}\int_{-\ell}^{+\ell}\frac{dz'\,d\varphi'}{\sqrt{(z-z')^2+4a^2\sin^2\frac{\varphi'}{2}}} \doteq \log\frac{4(\ell^2-z^2)}{a^2} \qquad (30)$$

ince

$$\int_{-\ell}^{\ell}\frac{dz'}{\sqrt{(z-z')^2+4a^2\sin^2\frac{\varphi'}{2}}} = \log\frac{(\ell-z)+\sqrt{(\ell-z)^2+4a^2\sin^2\varphi'/2}}{(\ell+z)+\sqrt{(\ell+z)^2+4a^2\sin^2\varphi'/2}}$$

$$\doteq \log\frac{\ell^2-z^2}{a^2\sin^2\frac{\varphi'}{2}}$$

nd

$$\frac{1}{2\pi}\int_{0}^{2\pi}\log\left(\frac{\ell^2-z^2}{a^2\sin^2\frac{\varphi'}{2}}\right)d\varphi' = \log\frac{4(\ell^2-z^2)}{a^2}$$

imilar approximations can be obtained by the integral

$$\int_{-\ell}^{\ell}\frac{dz'}{\sqrt{(z-z')^2+a^2}} = \log\frac{(\ell-z)+\sqrt{(\ell-z)^2+a^2}}{-(\ell+z)+\sqrt{(\ell+z)^2+a^2}} = \log\frac{4(\ell^2-z^2)}{a^2}+\delta(z) \qquad (31)$$

where

$$\delta(z) = \log\left\{\frac{1}{4}\left[\sqrt{1 + \left(\frac{a}{\ell - z}\right)^2} + 1\right]\left[\sqrt{1 + \left(\frac{a}{\ell + z}\right)^2} + 1\right]\right\}$$

which is small except when z is very close to the end of the wire.

Therefore, for thin wires, the linearized integral equation can be simplified by making the following approximation.

$$G_a(s,s') = \frac{1}{2\pi}\int_o^{2\pi} \frac{e^{-jkr(s,s',\varphi)}}{r(s,s',\varphi)}\, d\varphi = \frac{e^{-jkr_a}}{r_a} \qquad (32)$$

$$r_a = \sqrt{r_o^2 + a^2}$$

where

r_o is the linear distance between points p(o,o,s) and P'(o,o,s') and

a is the radius of the wire.

This approximation has given good results for thin cylindrical antennas, and it has been justified by the variational solution of this problem by Tai[12]. The linearized integral equation for the curved wires was derived with the thin wire approximation

$$ka \ll 1 \qquad \text{and} \qquad \ell \gg a$$

which also justifies the approximation introduced in Equation (32). We expect therefore to get some useful results with this approximation for the case of curved wire antennas.

2.5 Structures Which Give Closed Cycle Type Kernels

In general, the kernel function of the integral equation, which is derived from the free space Green's function, is symmetric with respect to the

source point and the observation point

$$K(x,x') = K(x', x) \tag{33}$$

But it is not Hermitian, for K(x,x') is a complex function and in general

$$\overline{K(x,x')} \neq K(x', x)$$

where $\overline{K}$ indicates the complex conjugate of K.

For the linearized integral equation, structures with translational symmetry, rotational symmetry and helicoidal symmetry give rise to a special type of kernel function

$$K_a(s,s') = K_a(|s-s'|) \tag{34}$$

where s and s' are points on the given curves. The kernel function of Equation (34) is known as the kernel of the closed cycle type, and it is sometimes called the difference kernel, or the convolution kernel. Geometrically, these structures are distinguished in that they are invariant under a one dimensional Abelian group of congruent transformation. The structures having this special property include straight wires, circular arcs and helical wires and no others. (See Appendix A)

All these structures give the following form for the Euclicean distance between two points s and s' on the curve

$$r_o(s,s') = r_o(|s-s'|) \tag{35}$$

Therefore, we have

$$\frac{\partial r_a}{\partial s} = - \frac{\partial r_a}{\partial s'}$$

and

$$N(s,s') = 1$$

Formula (17) is thus simplified to

$$M(s,s') = k^2 \left[(\hat{s} \cdot \hat{s}') - 1 \right] G_a(s,s') \qquad (36)$$

3. VARIATIONAL FORMULATION OF THE INPUT IMPEDANCE OF WIRE ANTENNAS

3.1 Derivation of the Variation Function

It was shown in the last chapter that the boundary value problem of a wire antenna can be formulated in terms of an integro-differential equation

$$-j\omega\epsilon \; E_t^{\,i}\,(s) = \frac{1}{4\pi}\int_{s_1}^{s_2} I(s')\left[\frac{\partial^2}{\partial s\partial s'} + k^2(\hat{s}\cdot\hat{s}')\right] G_a(s,s')\,ds' \qquad (6')$$

Symbolically, it can be written as

$$E = \mathbb{K}\, I \qquad (37)$$

where

$$E = E_t^{\,i}\,(s)$$

and

$\mathbb{K}$ is an integro-differential operator

$$\mathbb{K}\; I = \frac{1}{4\pi j\omega\epsilon}\int_{s_1}^{s_2} I(s')\left[\frac{\partial^2}{\partial s\partial s'} - k^2(s\cdot s')\right] G_a(s,s')\,ds'$$

The kernel K can be shown by the Lorentz Reciprocity Theorem, to have the symmetry property expressed by the following equality of inner products

$$< I_1, \mathbb{K}\, I_2 > = < I_2, \mathbb{K}\, I_1 > \qquad (38)$$

where

$$< I_1, \mathbb{K}\, I_2 > = \int_{s_1}^{s_2} (I_1\; \mathbb{K}\, I_2)\; ds \qquad (39)$$

Equation (39) is a bilinear from with an infinite number of variables, the corresponding quadratic form is called the Hilbert's double integral. It is known that when K is real and symmetric, the absolute value of the Hilbert double integral is bounded under the constraint

$$< I_1, I_1 > = 1$$

The kernel function $\mathbb{K}$, in our case, is complex symmetric. Instead of the above-mentioned property, the double integral can be shown to have a stationary point under the similar constraint condition.

When I_2, I_2 satisfies

$$\begin{aligned} E_1 &= \mathbb{K} I_1 \\ E_2 &= \mathbb{K} I_2 \end{aligned} \tag{40}$$

respectively, the function

$$Z_{12} = \frac{< I_1, \mathbb{K} I_2 >}{< E_1, I_2 > < E_2, I_1 >} \tag{41}$$

which gives the input impedance of an antenna when $E_1 = E_2$, is stationary.

This can be seen as follows.

When functions I_1 and I_2 vary, the first variation of Equation (41) can be written as

$$\delta Z_{12} = \frac{1}{< E_1, I_2 > < E_2, I_1 >} \left[\frac{< I_1, \mathbb{K} \delta I_2 > < E_1, I_2 > - < I_1, \mathbb{K} I_2 > < E_1, \delta I_2 >}{< E_1, I_2 >} \right.$$

$$\left. + \frac{< \delta I_1, \mathbb{K} \delta I_2 > < E_2, I_1 > - < I_1, \mathbb{K} I_2 > < E_2, \delta I_1 >}{< E_2, I_1 >} \right]$$

which vanishes when I_1 and I_2 satisfy Equation (40) and $\mathbb{K}$ has the property expressed by Equation (38).

The input impedance of a wire antenna, when referred to the input current $I(s_o)$, is defined as

$$Z_{in} = \frac{V}{I(s_o)} \tag{42}$$

where V is the voltage across the gap, and it can be expressed as

$$V = \int_{s_1}^{s_2} E_t^{\,i}(s)\, ds$$

for a δ-function excitation, we write $E_t^{\,i}(s) = V\,\delta\,(s-s_o)$. Then Equation (6') becomes

$$Z_{in}\; I(s_o)\;\delta\;(s-s_o) = \mathbb{K}\, I \tag{43}$$

multiplying both sides of Equation (43) by I and integrating between the limits s_1 to s_2, we obtain

$$Z_{in}\; I^2\,(s_o) = < I\, \mathbb{K}\, I >$$

hence

$$Z_{in} = \frac{< I\, \mathbb{K}\, I >}{I^2\,(s_o)} \tag{44}$$

Equation (44), which is a special case of Equation (41), has been shown to have the stationary property by Storer[8] for cylindrical antennas. Storer and Tai[9] have calculated the input impedance for these cylindrical antennas and the results checked closely with that obtained by King and Middleton[4] who used the Hallén's iterative method.

3.2 The First Order Solution and the Assumed Current Distribution

It is worthwhile to point out that the variational problem described in Chapter 3.1 is equivalent to the boundary value problem expressed by the integro-differential Equation (6). This equation can be considered as the Euler equation of the variation problem, in the sense that the variational formula is derived from the integro-differential equation and the integro-differential equation can be recovered from the variational formula by taking its first variation to be zero. The equivalence between these two problems is the basis of a method of solution to many physical problems. The well known Rayleigh-Ritz method is an example. For the solution of the Euler equation, one expands the unknown function in terms of a linear combination of known functions with unknown coefficients; the set of unknown coefficients are then determined by employing the stationary (or extremal) property of the variational formula.

In the wire antenna problem, the procedure consists of using the asymptotic solution of thin wire antennas as a zeroth order solution, for symmetric antennas, we write

$$I^{(o)}(s) = I_o i_o(s) = I_o \sin k(\ell - |s|) \tag{45}$$

where I_o is the amplitude of the current distribution and the zeroth order solution to this wire antennas is thus

$$Z^o_{in} = \frac{< i_o, \mathbb{K}' i_o >}{i_o^2(o)} \tag{46}$$

This leads to the same result as the EMF method.

The first order solution is obtained by adding a correction term to the zeroth order sinusoidal current distribution

$$I^{(1)}(s) = I_o\,[i_o(s) + A_1 i_1(s)] \qquad (47)$$

where $i_1(s)$ is a chosen function which satisfies the boundary condition required by $I(s)$ and A_1 is a variational parameter to be determined by the condition

$$\frac{\partial Z^{(1)}{}_{in}}{\partial A_1} = 0 \qquad (48)$$

In terms of the assumed current distribution functions, the input impedance formula can be written as

$$Z^{(1)}{}_{im} = j30\,\frac{\nu_1 + 2A_1\nu_2 + A_1^2\nu_3}{[i_o(o) + Ai_1(0)]^2} \qquad (49)$$

where

$$\nu_1 = \nu_{oo} = \frac{1}{k}\int_{s_1}^{s_2}\int_{s_1}^{s_2} i_o(s)\, i_0(s')\, \mathcal{K}_a\,(s,s')\, ds\, ds' \qquad (50$$

$$\nu_2 = \nu_{o1} = \frac{1}{k}\int_{s_1}^{s_2}\int_{s_1}^{s_2} i_o(s)\, i_1(s')\, \mathcal{K}_a(s,s')\, ds\, ds' = \nu_{10} \qquad (51)$$

$$\nu_3 = \nu_{11} = \frac{1}{k}\int_{s_1}^{s_2}\int_{s_1}^{s_2} i_1(s)\, i_1(s')\, \mathcal{K}_a(s,s')\, ds\, ds' \qquad (52)$$

and

$$\mathcal{K}_a(s,s') = \left[-\frac{\partial^2}{\partial s\partial s'} + k^2(\hat{s}\cdot\hat{s}')\right] G_a(s,s') \qquad (53)$$

To determine A_1, we differentiate $Z_{in}^{(1)}$ with respect to A_1 and set

$$\frac{\delta Z_{in}^{(1)}}{\delta A_1} = j60 \, \frac{[i_o(o) + A_1 i_1(o)][\nu_2 + A_1\nu_3] - [\nu_1 + 2A_1\nu_2 + A_1^2\nu_3]\, i_o(o)}{[i_o(o) + A_1 i(o)]^3} = 0$$

which gives

$$A_1 = \frac{i_1(o)\nu_1 - i_o(o)\nu_2}{i_o(o)\nu_3 - i_1(o)\nu_2} \tag{54}$$

Substituting Equation (54) in Equation (49) we have

$$Z_{in}^{(1)} = j30 \, \frac{\nu_1\nu_3 - \nu_2^2}{i_o^2(o)\nu_3 - 2i_o(o)i_1(o)\nu_2 + i_1^2(o)\nu_1} \tag{55}$$

For symmetric antennas, the choice of the function $i_1(s)$ made by Storer is

$$i_{1s}(s) = 1 - \cos k\,(\ell - |s|) \tag{56}$$

which gives rise to singularities in the input impedance for

$$k\ell = 2n\pi, \qquad n = 1,2,3.....$$

A better choice of the function was given by Tai[9]

$$i_{1T}(s) = k(\ell - |s|)\cos k(\ell - |s|) \tag{57}$$

3.3 Higher Order Solutions

For higher order solutions, we write, say for nth order.

$$I(s) = I_o[A_o i_o(s) + A_1 i_1(s) + \text{-----} + A_n i_n(s)] \tag{58}$$

without loss of generality, one can put $A_o = 1$. With Equation (58) we expand the impedance formula

$$Z. = \frac{j30}{I^2(o)} \int_{s_1}^{s_2} \int_{s_1}^{s_2} I(s)\, I(s')\, \mathcal{K}_a(s,s')\, ds\, ds'$$

and obtain

$$Z_{in}^{(n)} = j30 \frac{\sum_o^n \sum_o^n A_p A_q \nu_{pq}}{\left[\sum_o^n A_p i_p(o)\right]^2} \tag{59}$$

where

$$\nu_{pq} = \frac{1}{k} \int_{s_1}^{s_2} \int_{s_1}^{s_2} i_p(s)\, i_q(s')\, \mathcal{K}_a(s,s')\, ds'\, ds = \nu_{qp} \tag{60}$$

and the A_i's are determined by

$$\frac{\delta Z_{in}^{(n)}}{\delta A_i} = 0 \qquad i = 0,1,2,\text{-----}n \tag{61}$$

Equation (61) gives a set of equations as follows

$$\left[\sum_o^n A_p i_p(o)\right] \left[\sum_o^n A_p \nu_{pi}\right] - \left[\sum_o^n \sum_o^n A_p A_q \nu_{pq}\right] i_i(o) = 0 \tag{62}$$

$$i = 0,1,2,.....n$$

From Equations (62) and (59) we have

$$Z_{in}^{(n)}\left[\sum_{o}^{n} A_p\, i_p\,(o)\right] i_i(o) = j30 \sum_{o}^{n} A_p\, \nu_{pi} \tag{63}$$

$$i = 0,1,2,\ldots\ldots n$$

These are n + 1 equations for the set of variational parameters $\left\{A_i\right\}$ $i = 0,1,2,\ldots\ldots n$. To solve these equations, we first express the feeding condition

$$Z_{in}^{(n)} \sum_{o}^{n} A_p\, i_p\,(o) = \frac{V}{I_o} \tag{64}$$

where V is the given voltage difference at the input terminals, and thus Equation (63) becomes

$$\sum_{o}^{n} A_p\, \nu_{pi} = \frac{V\, i_i(o)}{j30\, I_o}$$

$$i = 0,1,2,\ldots\ldots n$$

In matrix form it can be written as

$$\bar{\bar{\nu}}\bar{A} = \frac{V}{j30\, I_o}\, \bar{i} \tag{65}$$

where

$$\bar{\bar{\nu}} = \begin{bmatrix} \nu_{oo} & \nu_{o1} & \cdots & \nu_{on} \\ \nu_{10} & \nu_{11} & \cdots & \nu_{1n} \\ \vdots & \vdots & & \vdots \\ \nu_{n0} & \nu_{n1} & \cdots & \nu_{nn} \end{bmatrix}$$

is a symmetric matrix and

$$\bar{A} = \begin{bmatrix} A_o \\ A_1 \\ | \\ | \\ | \\ | \\ A_n \end{bmatrix} \qquad \bar{i} = \begin{bmatrix} i_o(o) \\ i_1(o) \\ | \\ | \\ | \\ | \\ | \\ i_n(o) \end{bmatrix}$$

the solution of A is

$$\bar{A} = \frac{V}{j30\ I_o}\,\bar{\bar{\nu}}^{-1}\,\bar{i} \tag{66}$$

substituting Equation (66) into Equation (64), we obtain $Z_{im}^{(n)}$.

$$Z_{in}^{(n)} = j30\,\frac{1}{\bar{i}^{T}\,\bar{\bar{\nu}}^{-1}\,\bar{i}} \tag{67}$$

This reduces to the form (55) in the case of two parameters.

3.4 First Order Solution for Arc Antennas and Helical Antennas

In this section we shall apply the first order formula to some symmetrically curved wire antennas of half lenth ℓ, and curved wire antennas which we will consider are those which possess the closed cycle type kernel, namely, arc antennas and helical antennas, with cylindrical antennas as special cases.

The set of trial functions for the current distribution will be

$$i_o(s) = \sin k\,(\ell - |s|)$$

and

$$i_1(s) = k\,(\ell - |s|)\cos k\,(\ell - |s|)$$

For these antennas, the kernel function $\mathcal{K}_a(s,s')$ becomes

$$\mathcal{K}_a(|s-s'|) = \left(\frac{d^2}{ds^2} + k^2(\hat{s} \cdot \hat{s}')\right) G_a(|s-s'|) \tag{68}$$

This particular property can be used to simplify the set of double integrals ν_1, ν_2 and ν_3.

We first convert these integrals into the following forms.

$$\nu_1 = \frac{1}{k}\int_{-\ell}^{\ell}\int_{-\ell}^{\ell}\left[-\frac{di_o(s)}{ds}\,\frac{di_o(s')}{ds'} + k^2 f(s,s')\, i_o(s) i_o(s')\right] G_a(s,s')\, ds'\, ds \tag{69}$$

$$\nu_2 = \frac{1}{k}\int_{-\ell}^{\ell}\int_{-\ell}^{\ell}\left[-\frac{di_o(s)}{ds}\,\frac{di_1(s')}{ds'} + k^2 f(s,s')\, i_o(s) i_1(s')\right] G_a(s,s')\, ds'\, ds \tag{70}$$

$$\nu_3 = \frac{1}{k}\int_{-\ell}^{\ell}\int_{-\ell}^{\ell}\left[-\frac{di_1(s)}{ds}\,\frac{di_1(s')}{ds'} + k^2 f(s,s')\, i_1(s) i_1(s')\right] G_a(s,s')\, ds'\, ds \tag{71}$$

where

$$G_a(s,s') = \frac{e^{-jkr(s,s')}}{r(s,s')}$$

and

$$f(s,s') = (\hat{s} \cdot \hat{s}') \tag{72}$$

which is the cosine of the angle between the unit tangential vectors at s and s'. For helical antennas,

$$f(s-s') = \frac{1}{R_o^2 + b^2}\left[R_o^2 \cos\frac{s-s'}{\sqrt{R_o^2 + b^2}} + b^2\right] \tag{73}$$

$$r(s-s') = \left[4R_o^2 \sin^2\left(\frac{s-s'}{2\sqrt{R_o^2 + b^2}}\right) + b^2 \frac{(s-s)^2}{R_o^2 + b^2} + a^2\right] \qquad (74)$$

where

a is the radius of the wire

R_o is the radius of the helix

and

$$b = \frac{p}{2\pi}$$

where p is the pitch of the helix

For arc antennas

$$f(s-s') = \cos\frac{s-s'}{R_o} \qquad (75)$$

$$r(s-s') = \left[4R_o^2 \sin^2\left(\frac{s-s'}{2R_o}\right) + a^2\right] \qquad (76)$$

where

R_o is the radius of the circular arc and

a is the radius of the wire.

For symmetric antennas of these classes, ν_1, ν_2 and ν_3 can further be written as the following; for ν_2 we have

$$\nu_2 = \nu_{01} = \frac{2}{k}\int_o^{\ell}\int_o^{\ell}\left\{-\frac{di_o(s)}{ds}\frac{di_1(s')}{ds'}\left[G_a(s-s') - G_a(s+s')\right] + \right. \qquad (77)$$

$$\left. k^2 i_o(s) i_1(s') \left[f(s-s')\,G_a(s-s') + f(s+s')\,G_a(s+s')\right]\right\} ds'\,ds$$

with similar forms for ν_1 and ν_3. The double integrals of the form Equation (77) can readily be transformed into single integrals by using the following simple transformation

$$\begin{aligned} u &= s+s' \\ v &= s-s' \end{aligned} \tag{78}$$

First, we write the product of the trial functions in terms of new variables u and v

$$i_o(s)i_o(s') = \frac{1}{2}\,[\cos kv - \cos k(2\ell-u)] \tag{79}$$

$$i_o(s)i_1(s') = \frac{1}{4}\,k(2\ell-u+v)\,[\sin k(2\ell-u) - \sin kv] \tag{80}$$

$$i_1(s)i_1(s') = \frac{1}{8}\,k^2(2\ell-u+v)(2\ell-u-v)\,[\cos kv + \cos k(2\ell-u)] \tag{81}$$

Similarly, the product of derivations of trial functions can be expressed as follows

$$\frac{di_o(s)}{ds}\,\frac{di_o(s')}{ds'} = \frac{k}{2}\,[\cos kv + \cos k(2\ell-u)] \tag{82}$$

$$\frac{di_o(s)}{ds}\,\frac{di_1(s')}{ds'} = -\frac{k^3}{4}(2\ell-u+v)[\sin kv + \sin k(2\ell-u)] + \frac{k^2}{2}\,[\cos k(2\ell-u) + \cos kv] \tag{83}$$

$$\frac{di_1(s)}{ds}\,\frac{di_1(s')}{ds'} = \frac{k^4}{8}\,(2\ell-u+v)(2\ell-u-v)[\cos kv - \cos k(2\ell-u)] - \frac{k^3}{4}\,(2\ell-u-v)$$

$$[\sin k(2\ell-u)-\sin kv] - \frac{k^3}{4}\,(2\ell-u+v)\,[\sin k(2\ell-u) + \sin kv] + \frac{k^2}{2}\,[\cos kv + \cos k(2\ell-u)] \tag{84}$$

In u-v plane, double integrals ν_1, ν_2, and ν_3 can thus be written as single integrals (see Appendix B).

If we normalize the length in radians, i.e. let

$$L = k\ell$$

and with x = ku = kv as new variables, then the set of integrals ν_1, ν_2 and ν_3 become

$$\nu_1 = \int_0^L F_{11}(x)\ dx + \int_L^{2L} F_{12}(x)\ G(x)\ dx$$

$$\nu_2 = \int_0^L F_{21}(x)\ G(x)\ dx + \int_L^{2L} F_{22}(x) G(x)\ dx \qquad (85)$$

$$\nu_3 = \int_0^L F_{31}(x)\ G(x)\ dx + \int_L^{2L} F_{32}(x)\ G(x)\ dx$$

where

$$F_{11}(x) = [x \cos (2L-x) - 2(L-x) \cos x]\,[1-f(x)] + [2 \sin x - \sin (2L-x)][1+f(x)] \qquad (86)$$

$$F_{12}(x) = [1-f(x)]\,(2L-x) \cos (2L-x) + [1+f(x)] \sin (2L-x) \qquad (87)$$

$$F_{21}(x) = \left[\frac{3}{2}x - L - \left(L - \frac{x}{2}\right) f(x)\right] \cos (2\ell - x) + [1-f(x)]$$

$$\left[\left(\frac{x^2}{2} - Lx - \frac{1}{2}\right) \sin(2L-x) - (x^2 - xL - 1) \sin x\right] + [(3x-2L) + x\, f(x)] \cos x \qquad (88)$$

$$F_{22}(x) = (L-\frac{x}{2})\ [3 + f(x)]\cos(2L-x) - \left(\frac{x^2}{2} - 2Lx + 2L^2 - \frac{1}{2}\right)[1-f(x)]\sin(2L-x) \tag{89}$$

$$\begin{aligned} F_{31}(x) = {} & \left[(1-f(x))\left(-\frac{x^3}{6} + Lx^2 - L^2x + \frac{x}{2} - L\right) + x\right]\cos(2L-x) \\ & + \left[x^2 - 2Lx + (1+f(x)(-Lx+L^2-\frac{1}{2})\right]\sin(2L-x) \\ & + \left[-2x^2 + L(1-f(x))x + (1+L^2)(1+f(x))\right]\sin x \\ & + \left[(1-f(x))\left(\frac{-x^3}{3} + L^2x + x - \frac{2}{3}L^3\right) + 2x - 2L\right]\cos x \end{aligned} \tag{90}$$

$$\begin{aligned} F_{32}(x) = {} & \left[(1-f(x))\left(\frac{x^3}{6} - Lx^2 + 2L^2x - \frac{x}{2} - \frac{4}{3}L^3 + L\right) - x + 2L\right]\cos(2\ell-x) \\ & + \left[-x^2 + 4Lx - 4L^2 + \frac{1}{2} + \frac{1}{2}f(x)\right]\sin(2L-x) \end{aligned} \tag{91}$$

and where

$$f(x) = \frac{1}{c^2}\left[c_1^2\cos\frac{x}{c} + C_2^2\right] \tag{92}$$

$$G(x) = \frac{e^{-j\bar{r}(x)}}{\bar{r}(x)}$$

$$\bar{r}(x) = kr(u) = \left[4C_1^2\sin^2\left(\frac{x}{2c}\right) + 4C_2^2\left(\frac{x}{2C}\right)^2 + \epsilon^2\right]^{1/2} \tag{93}$$

with

$$\epsilon = ka$$

$$C_1 = kR_o$$

$$C_2 = kb$$

$$C = \sqrt{C_1^2 + C_2^2}$$

For arc antennas $C_2 = 0$

$$f(x) = \cos \frac{x}{C_1} \tag{94}$$

$$\bar{r}(x) = \left[4C_1^2 \sin^2\left(\frac{x}{2C_1}\right) + \epsilon^2\right]^{1/2} \tag{95}$$

and for cylindrical antennas $C_1 \longrightarrow \infty$

$$f(x) = 1$$

$$\bar{r}(x) = \left[x^2 + \epsilon^2\right]^{1/2} \tag{96}$$

The curvature of a helix can be expressed as

$$K = \frac{R_o}{R_o^2 + b^2}$$

and the normalized radius of curvature of the helix is thus

$$C_o = \frac{C_1^2 + C_2^2}{C_1} \tag{97}$$

The Equation (97) will be useful in describing some equivelent helical antennas which will be explained later.

4. COMPUTATIONAL RESULTS AND DISCUSSIONS

4.1 Computational Method

The numerical computations were carried out on ILLIAC, the digital computer of the University of Illinois. Some of the procedures used in computing the integrals and performing the algebraic operations of the impedance formula are described in Appendix C.

The computer program was prepared for computing the input impedances of helical antennas for a given set of parameters C_1, C_2, L and Ω . The first three parameters are the normalized physical dimensions of a helix, as defined previously.

$$C_1 = kR_o$$

$$C_2 = kb$$

$$L = k\ell$$

and Ω is defined as

$$\Omega = 2\ell n \frac{2\ell}{a}$$

For arc antennas, $C_2 = 0$. and for cylindrical antennas $C_2 = 0$, $C_1 = \infty$.

The computations for the input impedance of cylindrical antennas have been performed for

$\Omega = 8, 8.5, 9, 9.5, 10, 10.5, 11, 11.5, 12, 12.5, 13, 13.5, 14, 14.5, 15.$ While the parameter Ω was held constant ($\Omega = 10$) for the impedance computation for the arc antennas and the helical antennas. In case of the arc antennas, a series of computations were performed for the parameter C_1 in the range

$$0.5 \leq C_1 \leq 3.5$$

If the dimensions were such as to make the antenna arms meet, the computation outline would not be valid thus the largest values of L used in the computation were limited by the relation

$$L < \pi C_1$$

for a given value of C_1.

For helical antennas, the impedance computations were performed for the values of C_1 and C_2 in the following ranges.

$$0.3 \leq C_1 \leq 3$$

$$0.3 \leq C_2 \leq 2$$

4.2 The Input Impedances of Cylindrical Antennas

Although our main purpose was to evaluate the input impedances of curved wire antennas, particularly the arc antennas and the helical antennas, the impedance formula derived in Chapter 3 also gives the input impedances of cylindrical antennas. This will be discussed first for the following reasons.

(a) A cylindrical antenna is a special case of curved antennas. For curved wire antennas of small curvature, their input impedances approach that of cylindrical antennas. Furthermore, when $k\ell$ is small, the input impedance of all wire antennas should be practically the same. As $k\ell$ increases, the effect of the curvature begins to appear. The input impedance of a cylindrical antenna is therefore useful in extracting the effect of the curvature in the input impedance of a curved wire antenna.

(b) It is the nature of the approximation of the problem that it gives a better result for structures of relatively small curvature. Yet, we have no way of determining what exactly is the upper bound of the curvature

for which the approximation is still valid, there is no explicit condition for limiting values of C_1 and C_2 in the impedance formula. Hence in investigating the effect of curvature on the input impedances of these wire antennas, it is important for the purpose of comparison to compute the input impedances of the corresponding cylindrical antennas with the same method.

(c) The computing program can be checked by allowing the comparison of our results with published, experimentally confirmed data for the cylindrical antenna case.

(d) It will be shown later that in many respects the curved wire antenna behaves like a corresponding thinner cylindrical antenna.

In case of cylindrical antennas

$$f(x) = 1$$

The set of functions F_{ij}'s are simplified

$$F_{11}(x) = 4 \sin x - 2 \sin (2L - x)$$

$$F_{12}(x) = 2 \sin (2L - x)$$

$$F_{21}(x) = 2(X-L) \cos (2L - x) + 2(2x - L) \cos x$$

$$F_{22}(x) = 2(L - x) \cos (2L - x) \tag{98}$$

$$F_{31}(x) = x \cos (2L-x) + (x^2 - 4Lx + L^2 - 1) \sin (2L-x) + (-2x^2 + 2L^2 + 2) \sin x + (2x-L) \cos x$$

$$F_{32} (x) = (2L-x) \cos (2L - x) + (-x^2 + 4Lx - 4L^2 + 1) \sin (2L -x)$$

For the thin wires $ka \ll 1$, $\ell \gg a$ the following approximation is valid

$$\int \frac{e^{-j\bar{r}(x,\epsilon)}}{\bar{r}(x,\epsilon)}\,dx \doteq \int \frac{dx}{\bar{r}(x,\epsilon)} - \int \frac{1 - e^{-j\bar{r}(x,o)}}{\bar{r}(x,o)}\,dx$$

hen the set of integrals ν_1, ν_2, and ν_3 for cylindrical antennas can be xpressed in terms of known integrals, as given by Tai[9].

$${}_1 = -j\left\{2\mathcal{L}(2L) + e^{j2L}\left[\ell n\, 2 - \frac{\Omega}{2} - \mathcal{L}(4L) + 2\mathcal{L}(2L)\right] + e^{-j2L}\left[\frac{\Omega}{2} - \ell n 2\right]\right\}$$

$${}_2 = L\left[2-\Omega + \mathcal{L}(2L)\right] + e^{j2L}\left[L\left(-\frac{\Omega}{2} + 2\ell n 2 + 3\mathcal{L}(2L) - 2\mathcal{L}(4L)\right) - j\,\frac{1}{2}\right]$$

$$+ e^{-j2L}\left[L\left(-\frac{\Omega}{2} + 2\ell n 2\right) + j\,\frac{1}{2}\right] \qquad (99)$$

$${}_3 = \left[-j\mathcal{L}(2L) + L\left(-\frac{1}{2} - \Omega + \mathcal{L}(2L)\right) - jL^2\left(-\frac{1}{2} + \mathcal{L}(2L)\right)\right]$$

$$+ e^{j2L}\left[j\frac{1}{4}\left(-\frac{1}{2} - 2\,\ell n 2 + \Omega - 4\mathcal{L}(2L) + 2\mathcal{L}(4L)\right) + L\left(1 + \ell n 2 + \mathcal{L}(2L) - \mathcal{L}(4L)\right)\right.$$

$$\left. + jL^2\left(2\ell n 2 - \frac{1}{2}\Omega + 3\mathcal{L}(2L) - 2\mathcal{L}(4L)\right)\right] + e^{-j2L}\left[j\,\frac{1}{4}\left(\frac{1}{2} - 2\ell n\, 2 - \Omega\right)\right.$$

$$\left. + L(1 + \ell n 2) + jL^2\left(-\frac{1}{2} - 2\ell n 2 + \frac{1}{2}\Omega\right)\right]$$

ere

$$\Omega = 2\ell n \frac{2\ell}{a}$$

and

$$\mathcal{L}(L) = \int_0^L \frac{1 - e^{-jx}}{x} \, dx \tag{100}$$

which can be expressed in terms of sine and cosine integrals.

The input impedance of cylindrical antennas has been calculated for the following values of the parameters.

a. $k\ell = 1.5 \longrightarrow 3.7$ $\Omega = 8 \longrightarrow 15$

b. $k\ell = 4.7 \longrightarrow 6.9$ $\Omega = 11.5 \longrightarrow 15$

c. $k\ell = 7.9 \longrightarrow 9.9$ $\Omega = 12 \longrightarrow 15$

These results are presented in Figure 6, Figure 7 and Figure 8, respectively. For wire antennas, thier impedance characteristics resemble that of a lossy transmission line; the impedance curve plotted in a rectangular chart would circle around a point which represents the characteristic impedance of the structure. For this reason, the impedance curves of wire antennas are sometimes called circular graph.

In these figures, the dotted lines indicated the equi-$k\ell$ contours. For $\Omega = 10$ and 15, our results coincide with that given by Tai and Storer.

The properties of the input impedances of cylindrical antennas have been in great detail by King[13]. We shall put down only a few useful definitions and mention some notable effects to facilitate the discussion for the input impedances of curved wire antennas.

The terms, input resonance and input anti-resonance, will be used as in the following defined sense.

1. Input resonance is characterized by

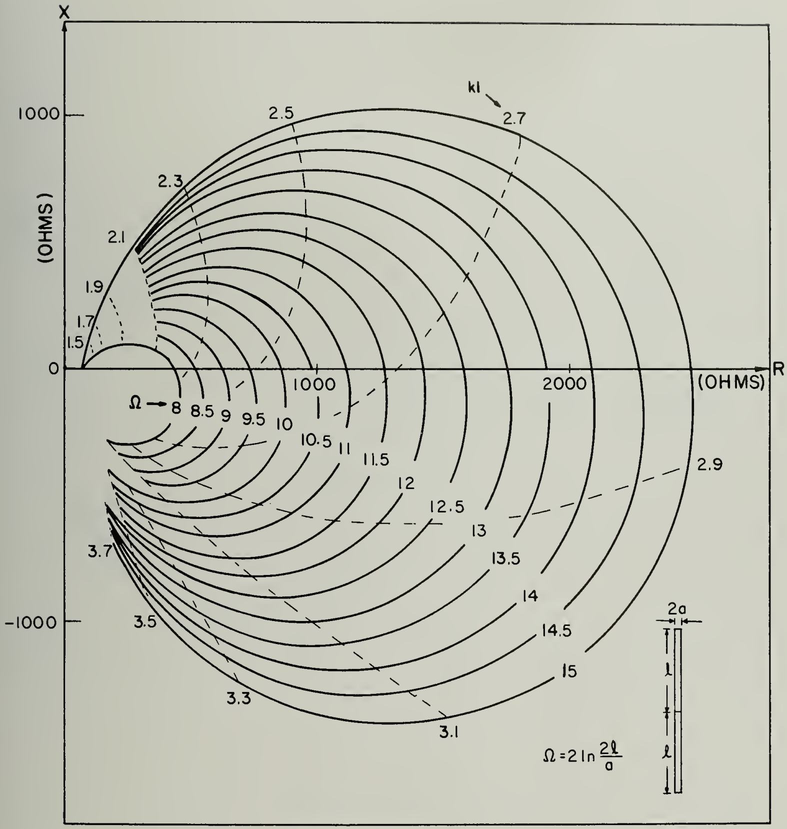

Figure 6. The Input Impedances of Cylindrical Antennas (kl = 1.5 to 3.7)

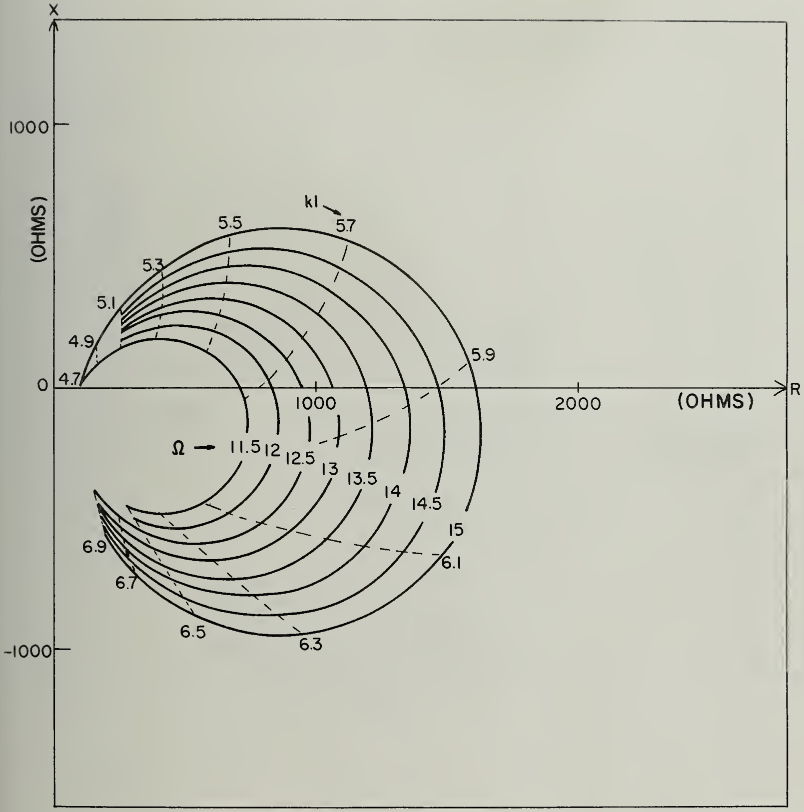

Figure 7. The Input Impedances of Culindrical Antennas
(kl = 4.7 to 6.9)

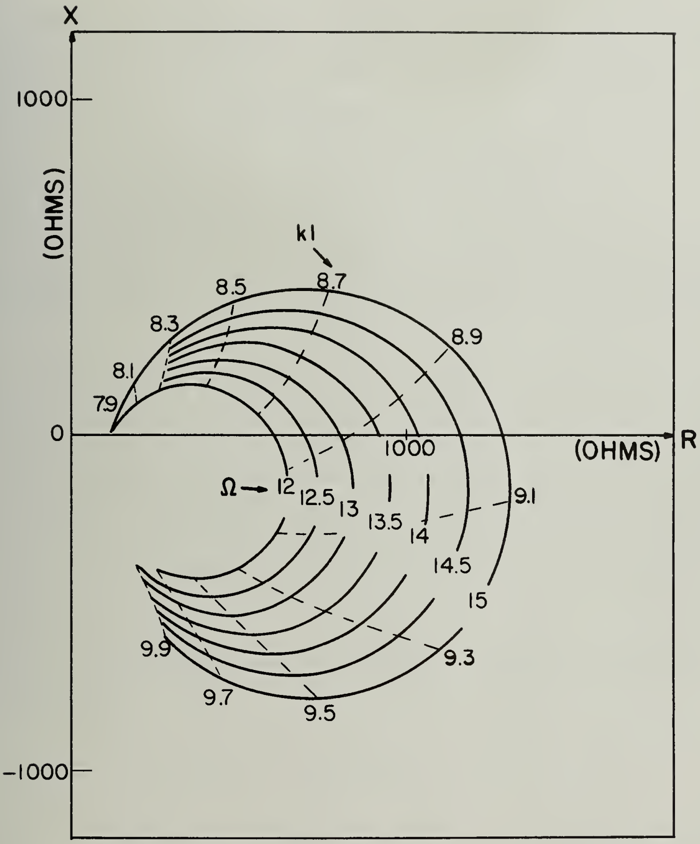

Figure 8. The Input Impedances of Cylindrical Antennas
(kl = 7 9 to 9.9)

a) The reactive part of the input impedance vanishes

b) $k\ell = (k\ell)$ res is near $n\pi/2$ with $n = 1,3,5...$

The resistive part of the input impedance in this case will be called the resonant resistance, (R) res and $(k\ell)$ res, the resonant length.

2. Input antiresonant is characterized by

a) The reactive part of the input impedance vanishes

b) $k\ell = (k\ell)$ antires is near $n\pi/2$ with $n = 2, 4, 6.....$

The resistive part of the input impedance in this case will be called the antiresonant resistance, (R) antires and $(k\ell)$ antires, the antiresonant length.

It is known that for cylindrical antennas, (R) res decreases as Ω increases. This indicates that for a same input current the thinner wire radiates less power at their resonant lengths, also at these lengths the thinner wire has more stored energy. The quality factor Q of a cylindrical antenna increases as Ω increases at the resonant length. On the other hand (R) anti–res increases as Ω increases.

Another known fact for cylindrical antennas is that the formula for the natural wavelengths

$$\lambda_n = \frac{4\ell}{n}, \qquad n = 1,2,3.....$$

is valid only for wires of the infinitesimal size. For finite size conductors, it is replaced by

$$\lambda_n = \frac{4(\ell + \delta)}{n}, \qquad n = 1,2,3.....$$

where δ is always greater than zero and decreases as Ω increases. The shortening of resonant lengths and antiresonant length are expressed by

$$\alpha_n = \frac{n\pi}{2} - (k\ell)\text{res} > 0 \qquad n = 1,3,5.....$$

$$\beta_n = \frac{n\pi}{2} - (k\ell)\text{ anti-res} > 0 \qquad n = 2,4,6.....$$

Furthermore, it is seen from the circular graphs of the input impedance (Figures 6 through 8) that

α_1 decreases as Ω increases, i.e. $(k\ell)$ res is larger for thinner wires.

β_n also decreases as Ω increases; i.e. $(k\ell)$ anti-res is larger for thinner wires.

4.3 The Input Impedance of Arc Antennas

In order to see the effect of the curvature, we computed the input impedance of arc antennas with constant $\Omega = 10$ and $C_2 = 0$. A series of impedance graphs were obtained by varying the parameter C_1, i.e. $2\pi R_o/\lambda$, the circumference in wavelength.

The half length of the arc antenna, ℓ, is limited for a given R_o by the relation

$$\ell < \pi R_o \qquad \text{or} \qquad k\ell < \pi C_1$$

The input impedances for $C_1 = 0.5$ to 3.5, together with the input impedances of the corresponding cylindrical antenna are shown in Figure 9. The dotted lines are contours of equal length (equi $k\ell$).

It is seen that the larger the curvature of the arc antenna, the larger is the circular graph of its input impedance. This enlargement effect of the circular graph for arc antennas is very similar to the effect for cylindrical

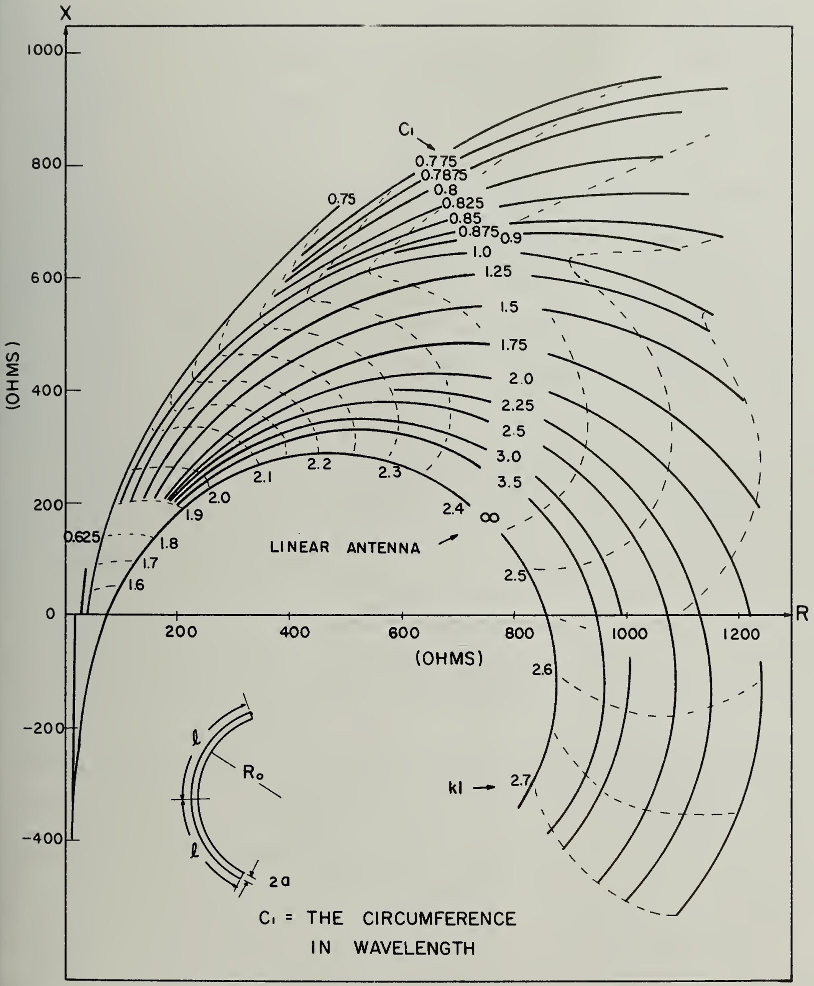

Figure 9. The Input Impedances of Arc Antennas

antennas as we increase Ω, i.e., decreasing the thickness of the wire, in which case the thinner wire has lower resonance resistance and higher anti-resonance resistance. In the case of arc antennas of the same thickness the curvature produces a similar effect on the input impedance as that due to the thickness of cylindrical antennas. Therefore the curved antenna has a lower resonance resistance and yet a higher anti-resonance resistance. Resonant resistances, (R)res, range from 17 ohms for $C_1 = 0.5$ to 70 ohms for $C_1 = 3.5$ (Figure 10). While antiresonance resistances, (R) antires, range from 945 ohms for $C_1 = 3.5$ to 1800 ohms for $C_1 = 0.875$ (Figure 11). For smaller values of C_1, the antenna arms do not reach the resonant and the antiresonant length, respectively, before meeting each other.

The resonant length, $(k\ell)$ res and the antiresonant length, $(k\ell)$ antires as a function of the normalized radius of curvature as shown in Figure 12. The shortening effect expressed by

$$\alpha = \frac{\pi}{2} - (k\ell)\text{res}$$

$$\beta = \pi - (k\ell)\text{ antires}$$

are shown in Figure 13 as a function of the normalized radius of curvature for the arc antennas. The variation of these lengths have maximums at $C_1 = 1.175$ for the anti resonant lengths and at $C_1 = 0.575$, for the resonant length. The former corresponds to the structure $2\pi R_o = 1.175\ \lambda$ and later corresponds to $2\pi R_o = 0.575\ \lambda$. This particular effect was observed by Englund[10] in 1928 when he performed some measurements on the natural period of curcular arcs of various radii of curvature. He obtained an extremum in his measured values of the ratio of resonant wavelength to arc length. The

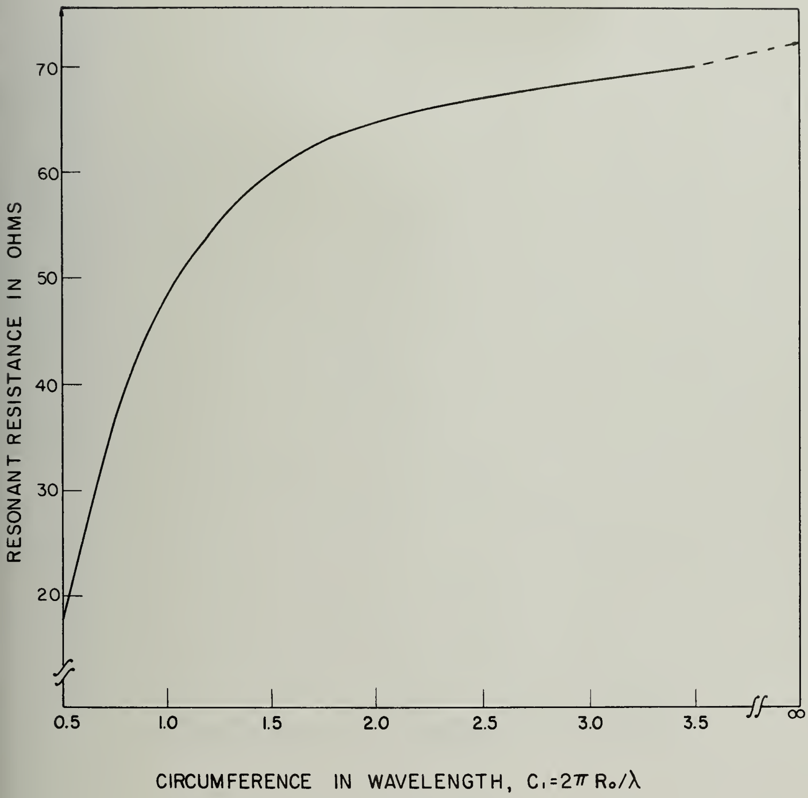

Figure 10. Resonant Resistances of Arc Antennas

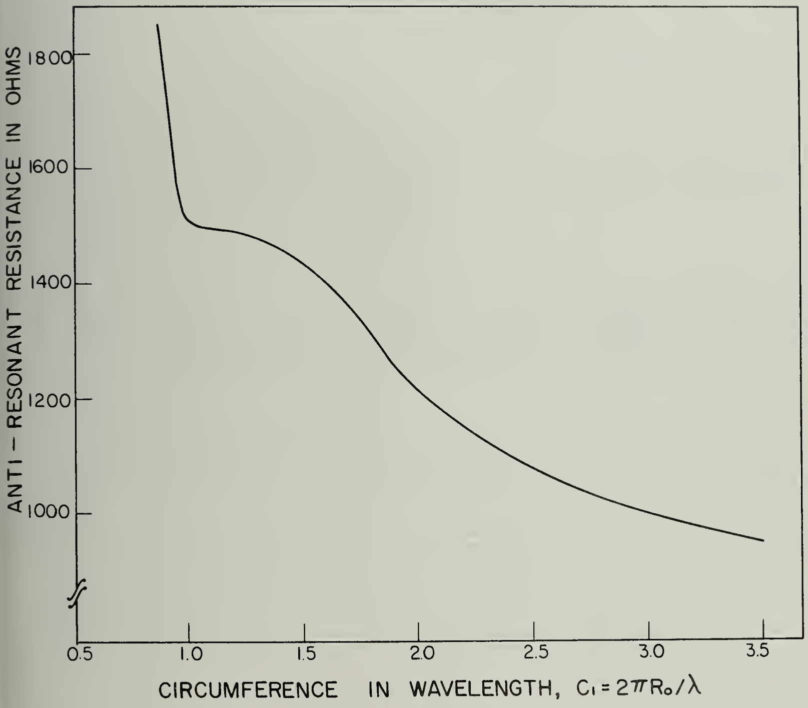

Figure 11. Antiresonance Resistances of Arc Antennas

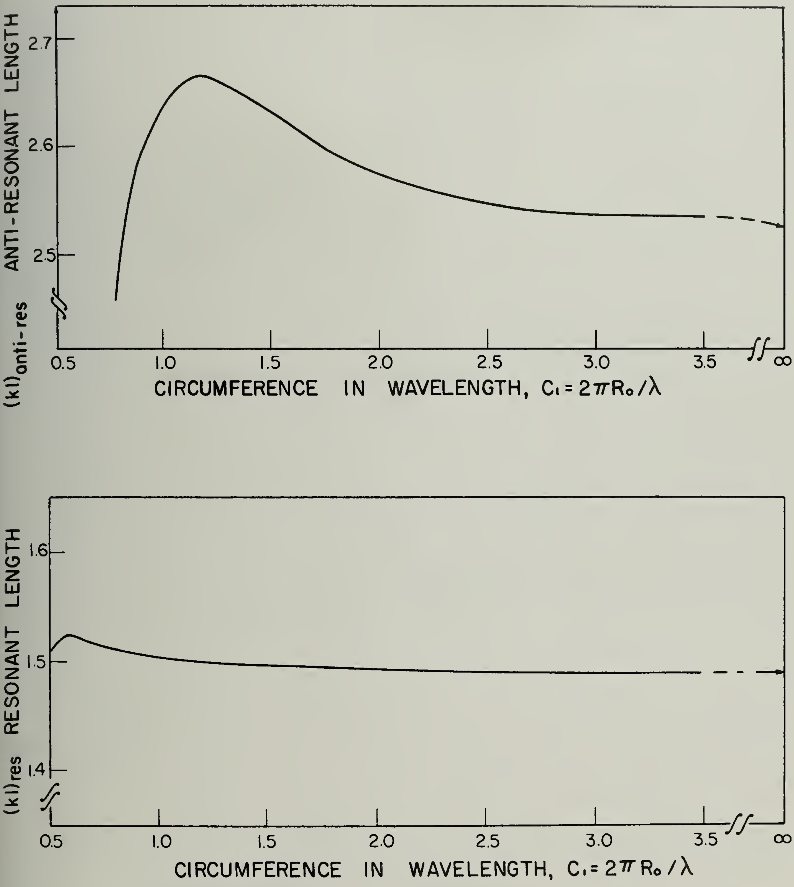

Figure 12. Resonant Lengths and Antiresonant Lengths for Arc Antennas

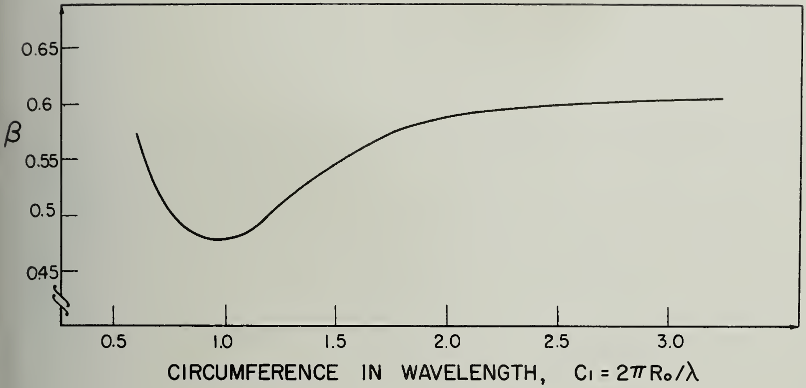

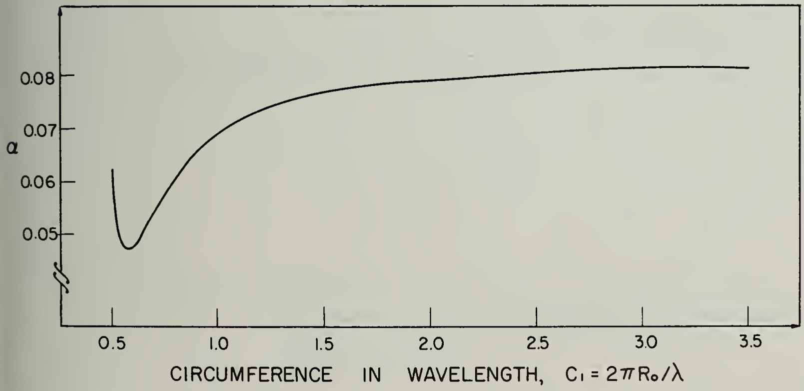

Figure 13. Shortenings of Resonant Length and Antiresonant Length of Arc Antennas

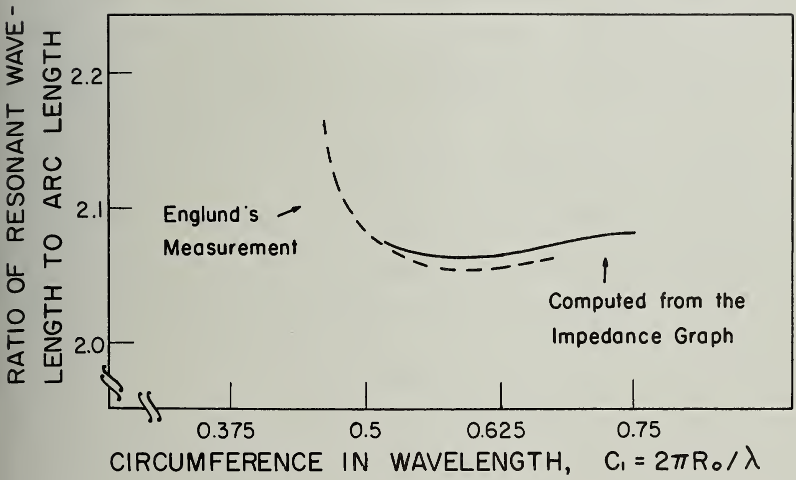

Figure 14. The Ratio of Resonant Wavelength to Arc Length as a Function of C_1 -- Comparison Between Englund's Measured Results and That Obtained from the Impedance Graphs

computed result from the impedance graph give values of $\left(\frac{\lambda}{2\ell}\right)$res very close to Englund's measured values (Figure 14). In both results, the extremum occur at $C_1 = 0.575$.

The variation of the resonant resistance, (R) res, and the antiresonant resistance, (R) antires, and also those of the resonant length, $(k\ell)$ res, and the antiresonant length, $(k\ell)$ antires, can be divided into two regions of different characteristics. For structures of large curvature, the variation shows a larger slope and becomes slowly varying in the region where the curvature of the structure is small.

In the resonance case, the length of the antenna is short, and the effect of the curvature increases gradually as we decrease C_1. For small values of C_1 where the arms of a resonant antenna almost meet each other, the effect of the curvature increases much more appreciably.

TABLE I

C_1	0.5	0.75	1	1.5	2	2.5	3	3.5
πC_1	1.57	2.36	3.14	4.71	6.28	7.85	9.43	11
$(k\ell)$res	1.508	1.513	1.501	1.493	1.4905	1.4985	1.489	1.4885
$(k\ell)\text{res}/\pi C_1$	0.96	0.642	0.478	0.317	0.238	0.19	0.158	0.135

Table I gives the resonant length in terms of the half circumference length of the loop, all in radians for $(k\ell)\text{res}/\pi C_1 > 0.5$ where $C_1 < 1$. There is more variation in the curves of (R)res and $(k\ell)$res than in that for the region $(k\ell)\text{res}/\pi C_1 < 0.5$, where $C_1 > 1$. The set of corresponding values of $(k\ell)$antires and πC_1 are shown in Table II.

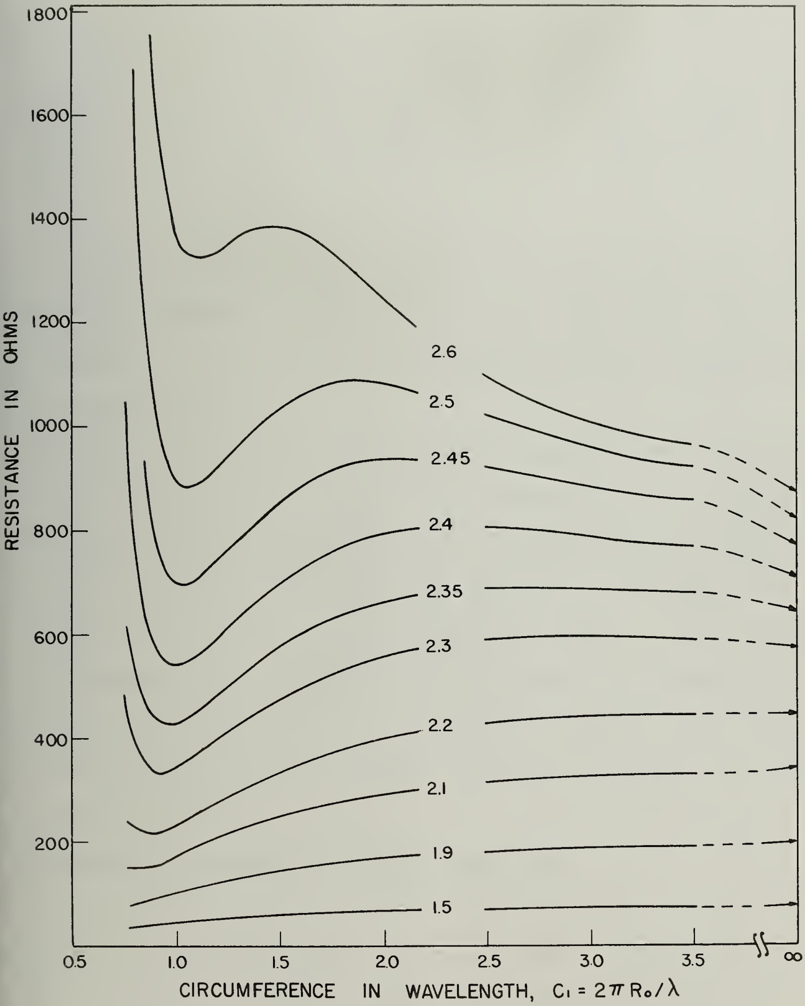

Figure 15. Resistive Part of the Input Impedance Along Equi-$k\ell$ Contours

TABLE II

C_1	0.875	1	1.25	1.5	2	2.5	3	3.5
πC_1	2.65	3.14	3.93	4.71	6.28	7.96	9.43	11
$(k\ell)$antires	2.58	2.64	2.66	2.63	2.57	2.55	2.54	2.536
$\frac{(k\ell)\text{antires}}{\pi C_1}$	0.938	0.844	0.703	0.58	0.409	0.32	0.269	0.211

Again, for higher values of the ratio $(k\ell)$antires/πC_1 the curves of (R)antires and $(k\ell)$antires change more rapidly. Particularly, there appears a resonant phenomena at $e_1 = 1$, i.e. when the circumference of the loop $2\pi R_o$ equals to one wavelength ($2\pi R_o = \lambda$).

The values of the resistance along various equi-$k\ell$ contours are plotted in Figure 15. For small $k\ell$, the variation is small except for $C_1 < 2$. As $k\ell$ increases, the resistances along the equi-$k\ell$ contour show more variation. For $k\ell > 2.2$, the curves begin to give a minimum in the neighborhood of $C_1 = 1$. This minimum shifts toward larger C_1 for larger $k\ell$. There is also a maximum in these curves which moves toward smaller C_1 as shown in the figure. These maximum and minimum effects of the resistance and the extremum effect observed by Englund are closely related, yet they are difficult to explain in terms of simple physical reasonings.

4.4 Electromagnetic Resonance of Thin Wire Conductors

The resonant wavelengths and quality factors of thin wire conductors can be determined by equating the stored electric and magnetic energies of the system[11]. Since the loss of power by radiation has only a second-order effect on the natural frequencies, the formulation is essentially on the static basis.

Associated with the current distribution on the wire there is certain quantity ϵ_m of stored magnetic energy

$$\epsilon_m = \frac{\mu}{8\pi}\iint r^{-1}\, I(s)I(s')\,(\hat{s}\cdot\hat{s}')\,ds'\,ds = \frac{\mu}{8\pi} < I\,\mathbb{K}_m\,I > \qquad (101)$$

$$\mathbb{K}_m = (\hat{s}\cdot\hat{s}')/r$$

Similarly, associated with the charge distribution the stored electric energy is

$$\epsilon_e = \frac{1}{8\pi\epsilon}\iint r^{-1}\, q(s)q(s')\,ds'\,ds = \frac{1}{8\pi\epsilon} < q\,\mathbb{K}_e\,q > \qquad (102)$$

$$\mathbb{K}_e = 1/r$$

by the equation of continuity ϵ_e can be written as

$$\epsilon_e = \frac{1}{8\pi\epsilon\omega^2} < I'\,\mathbb{K}_e\,I' >$$

where ω is a natural frequency.

Equating the Equations (101) and (102), we obtain the formula

$$\omega^2\mu\epsilon = \left(\frac{2\pi}{\lambda}\right)^2 = \frac{< I'\,\mathbb{K}_e\,I' >}{< I\,\mathbb{K}_m\,I >} = \frac{\mathbb{I}_e}{\mathbb{I}_m} \qquad (103)$$

For thin wires, the double integrals in Equation (103) can be written as

$$\mathbb{I}_e = < I'\,\mathbb{K}_e\,I' > \doteq \iint [I'(s)]^2\,\mathbb{K}_e(s,s')\,ds'\,ds$$

$$\mathbb{I}_m = < I\,\mathbb{K}_m\,I > \doteq \iint [I(s)]^2\,\mathbb{K}_m(s,s')\,ds'\,ds$$

The approximation is justified for thin wires due to the large contribution of the integrand at the neighborhood of $s = s'$.

To evaluate resonant wavelength and the quality factor Q, we assume

$$I(s) = I_o \sin \frac{n\pi}{2\ell} s = I_o\, i(s)$$

where 2ℓ is the antenna length. From Equation (103), we have

$$\frac{2\pi}{\lambda_n} = \left[\frac{< i' \mathcal{K}_e\, i' >}{< i \mathcal{K}_m\, i >}\right]^{1/2} = \left[\frac{\Pi_e}{\Pi_m}\right]^{1/2} \qquad (104)$$

and the quality factor Q_n associated with the nth natural mode can be expressed as

$$Q_n = \frac{60\pi}{\lambda_n R_n} < i \mathcal{K}_m\, i > = \frac{30}{R_n} [< i \mathcal{K}_m\, i > < i' \mathcal{K}_e\, i' >]^{1/2} = \frac{30}{R_n} [\Pi_e \Pi_m]^{1/2}$$

when R_n is the radiation resistance referred to a current antinode.

For cylindrical antennas, we have

$$\Pi_e^o = \frac{1}{2}\, \frac{n\pi}{2\ell}\, [\Delta - s_i\, (2n\pi)]$$

$$\Pi_m^o = \frac{1}{2}\, \frac{2\ell}{n\pi}\, [\Delta + s_i\, (2n\pi)]$$

where

$$\Delta = 2n\pi \left[\frac{\Omega}{2} + \log 2 - 1\right]$$

and s_i is a sine integral. For arc antennas, we write

$$\Pi_e = \Pi_e^o + \delta\Pi_e$$

$$\Pi_m = \Pi_m^o + \delta\Pi_m$$

and

$$\delta\Pi_e \cong \frac{1}{24}\frac{1}{R_o^2} < i' \frac{v^2}{r_o} i' > = \frac{-1}{12}\frac{1}{R_o^2}\ell$$

$$\delta\Pi_m \cong -\frac{11}{24}\frac{1}{R_o^2} < i \frac{v^2}{r_o} i > = \frac{11}{3}\frac{1}{R_o^2}\frac{\ell^3}{(n\pi)^2} (1 + 2 \cos n\pi) \tag{106}$$

For n = even

$$\delta\Pi_m = 11 \frac{1}{R_o^2}\frac{\ell^3}{(n\pi)^2}$$

for n = odd

$$\delta\Pi_m = -\frac{11}{3}\frac{1}{R_o^2}\frac{\ell^3}{(n\pi)^2}$$

Therefore, it is seen that in comparison to cylindrical antennas $(k\ell)$res becomes larger for arc antennas and helical antennas while $(k\ell)$antires becomes smaller for curved structures. Since

$$(k\ell)\text{res} = \frac{n\pi}{2}\sqrt{\frac{\Delta - s_i(2n\pi)}{\Delta + s_i(2n\pi)}}\left[1 + \frac{5}{3}\frac{\ell^2}{\Delta R_o^2 n\pi}\right] \tag{107}$$

$$n = 1,3,5.....$$

and

$$(k\ell)\text{antires} = \frac{n\pi}{2}\sqrt{\frac{\Delta - s_i(2n\pi)}{\Delta + s_i(2n\pi)}}\left[1 - \frac{17}{3}\,\frac{\ell^2}{\Delta R_o^2 n\pi}\right] \qquad (108)$$

$$n = 2,4,6.....$$

They therefore agree with that indicated in Figure 9 for $kR_o > 2.5$. The approximation for deriving Equation (103) holds only for relatively small curvatures.

For the quality factor Q, we have, From Equation (105)

$$Q_{res} = \frac{15}{R_n}\sqrt{[\Delta - s_i(2n\pi)][\Delta + s_i(2n\pi)]}\left[1 - \frac{\ell^2}{\Delta R_o^2 n\pi}\right] \qquad (109)$$

$$n = 1,3,5.....$$

and

$$Q_{antires} = \frac{15}{R_n}\sqrt{[\Delta - s_i(2n\pi)][\Delta + s_i(2n\pi)]}\left[1 + \frac{16}{3}\,\frac{\ell^2}{\Delta R_o^2 n\pi}\right] \qquad (110)$$

$$n = 2,4,6.....$$

Q_{res} is larger for curved structures while $Q_{antires}$ is larger for cylindrical antennas, since R_n at resonance decreases as the curvative is increased at a faster rate than the decrement due to the term $\ell^2/\Delta R_o^2 n\pi$. At antiresonance R_n increases as the curvature is increased and its order is also higher than the increment due the term $\frac{16}{3}\ell^2/\Delta R_o^2 n\pi$.

The results obtained from this analysis agree qualitatively with those obtained from the input impedance graphs. Quantitatively speaking, the discrepancy between these two results exist even for the cylindrical antenna

case. This, perhaps, is due to the different assumption on the current distribution.

4.5 The Input Impedances of Helical Antennas

For helical antennas, input impedances were calculated as functions of C_1 and C_2 with $\Omega = 10$, where

$$C_1 = kR_o, \qquad R_o \text{ is the radius of the helix}$$

$$C_2 = kb, \qquad b = \frac{p}{2\pi}, \ p \text{ is the pitch of the helix}$$

Results are presented in the form of circular graphs. Figures 16, 17, and 18 give the input impedances of helical antennas of constant C_1 ($C_1 = 0.5$, $C_1 = 0.75$ and $C_1 = 1$), while Figure 21a and 21b give the input impedances of constant pitch helical antennas for which $C_2 = 0.25$ and Figure 22 is that for $C_2 = 0.5$.

When the size of the helix is fixed and the pitch is varied, the circular graph of the input impedance enlarges as we decrease the pitch. The input impedance of the helical antennas approaches that of the arc antenna for the small pitch and approaches that of the cylindrical antenna for the large pitch as expected. The range between these two limits is a function of C_1, namely the size of the helix in wavelengths. The range is larger for smaller C_1 and is narrowed down to zero for large values of C_1. The rate of this convergence is shown in Figure 19 and Figure 20. Figure 19 is the variation of the resonant resistance as a function of C_2 and with C_1 as a parameter while Figure 20 indicates that of the antiresonant resistance.

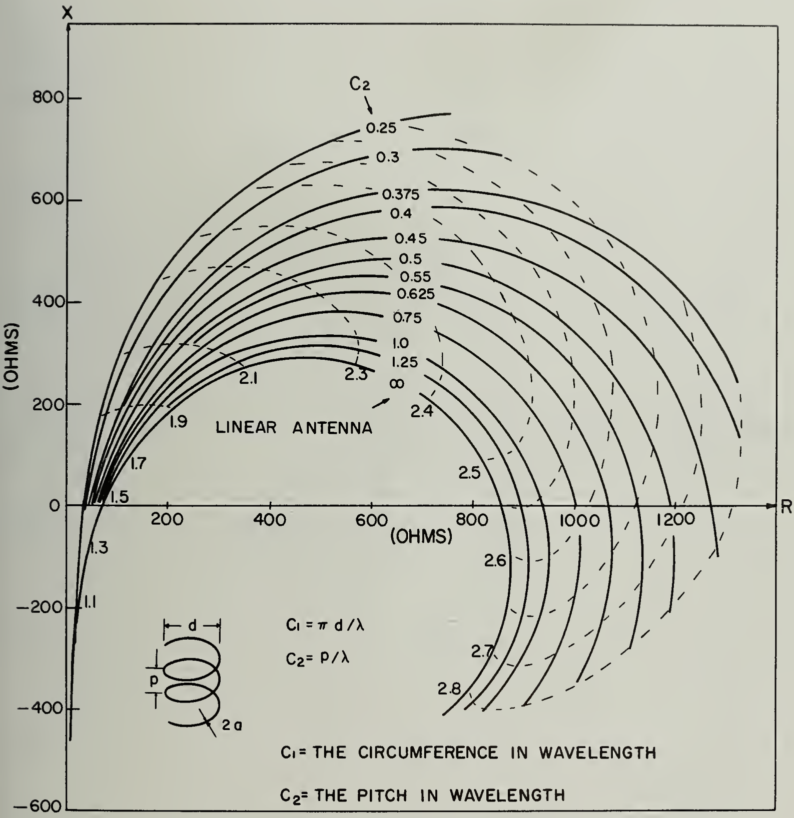

Figure 16. The Input Impedances of Helical Antennas $C_1 = 0.5$

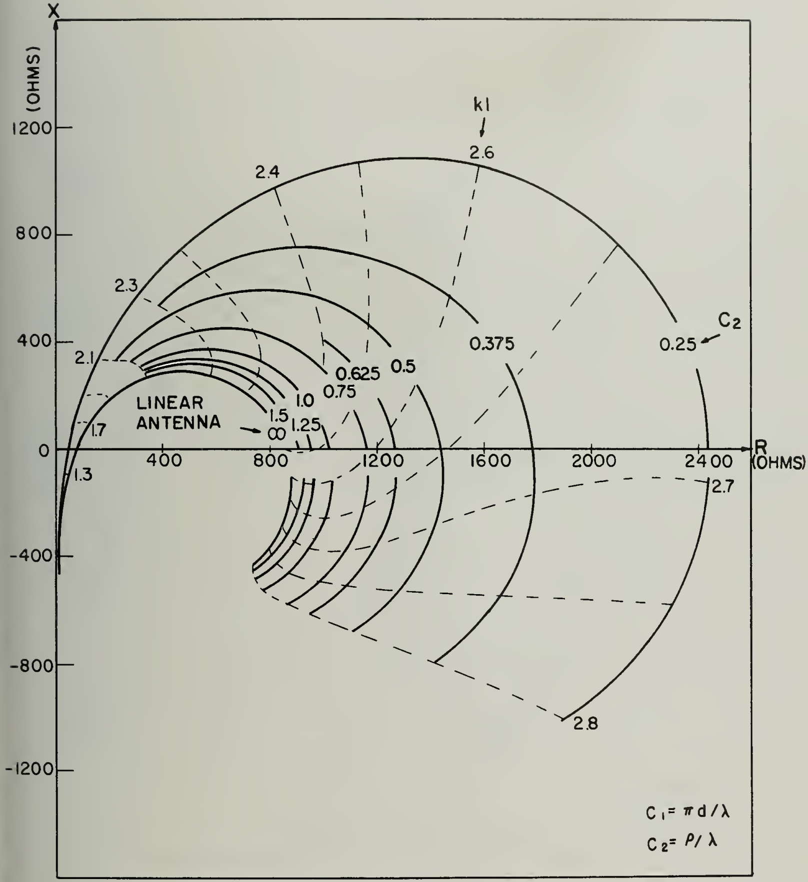

Figure 17. The Input Impedances of Helical Antennas $C_1 = 0.75$

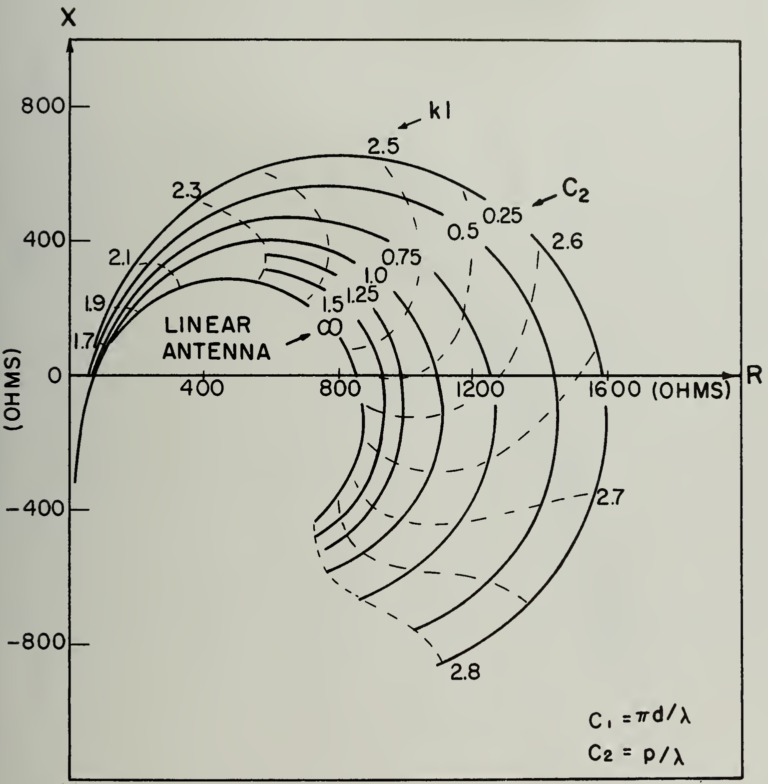

Figure 18. The Input Impedances of Helical Antennas $C_1 = 1$

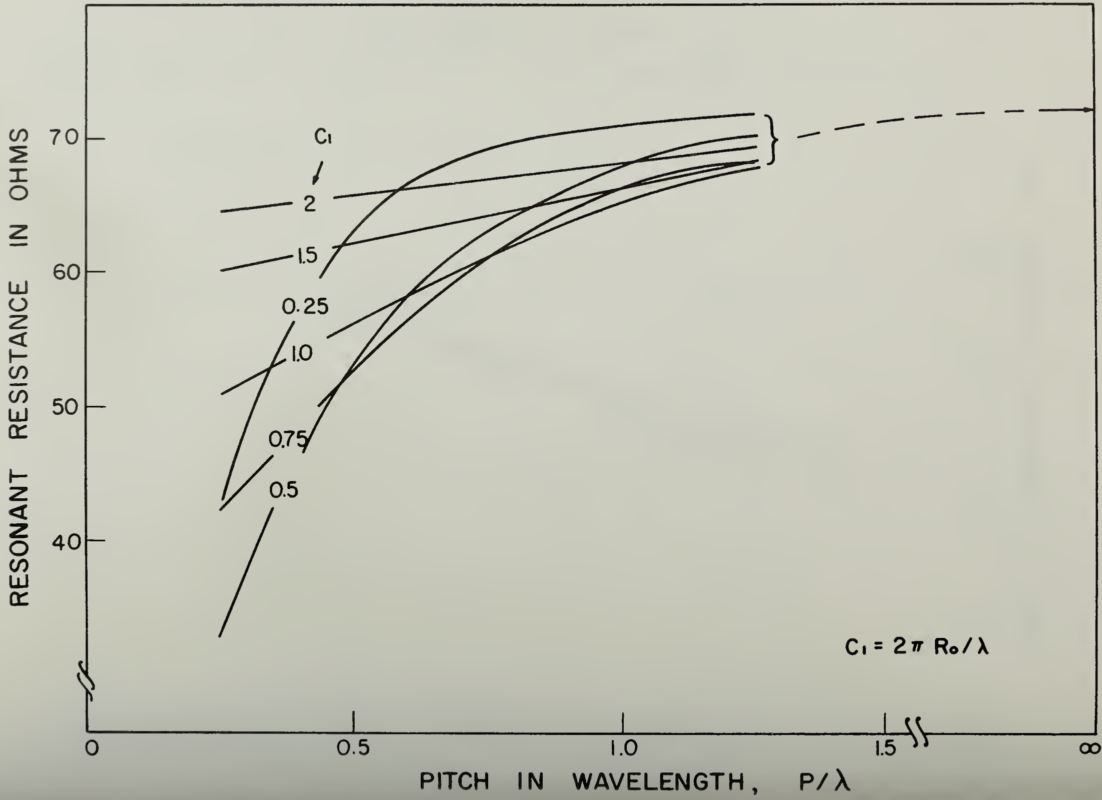

as a function of Pitch in Wavelength

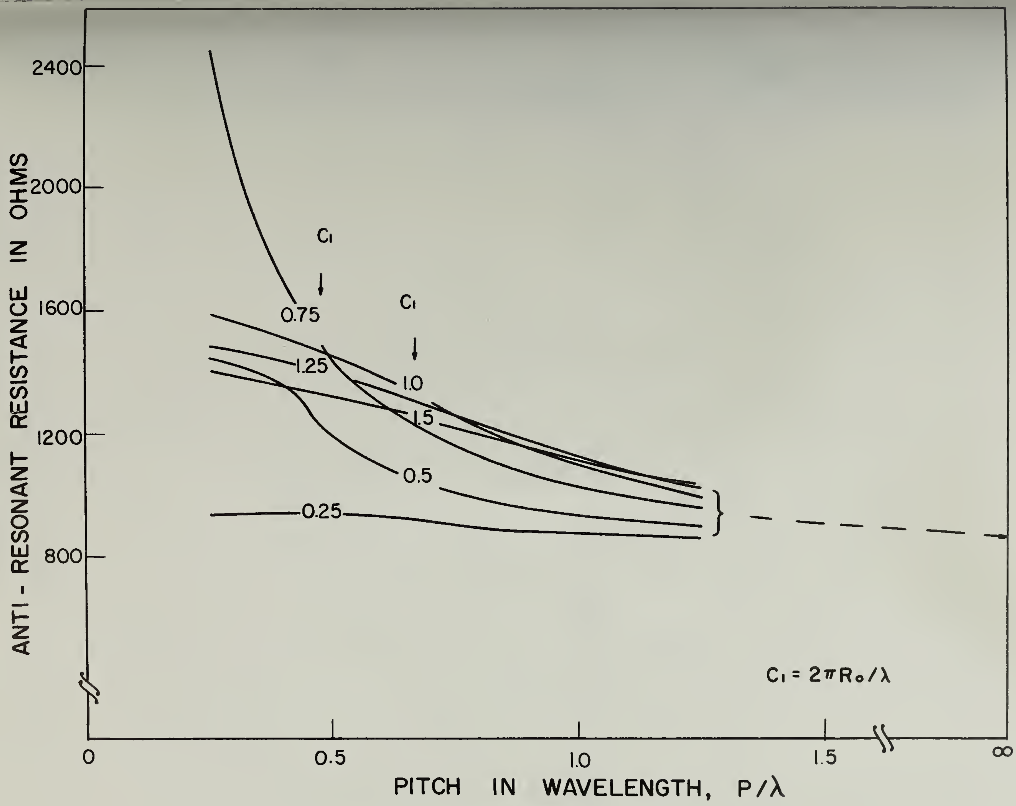

Figure 20. Antiresonant Resistance as a Function of Pitch in Wavelength

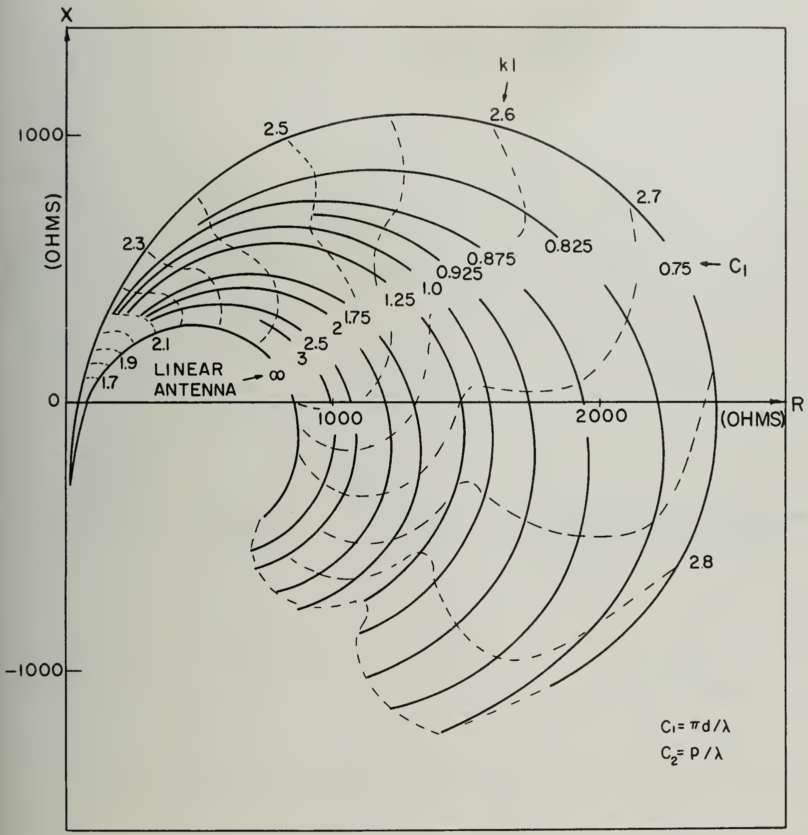

Figure 21a. The Input Impedances of Helical Antennas
$C_2 = 0.25$

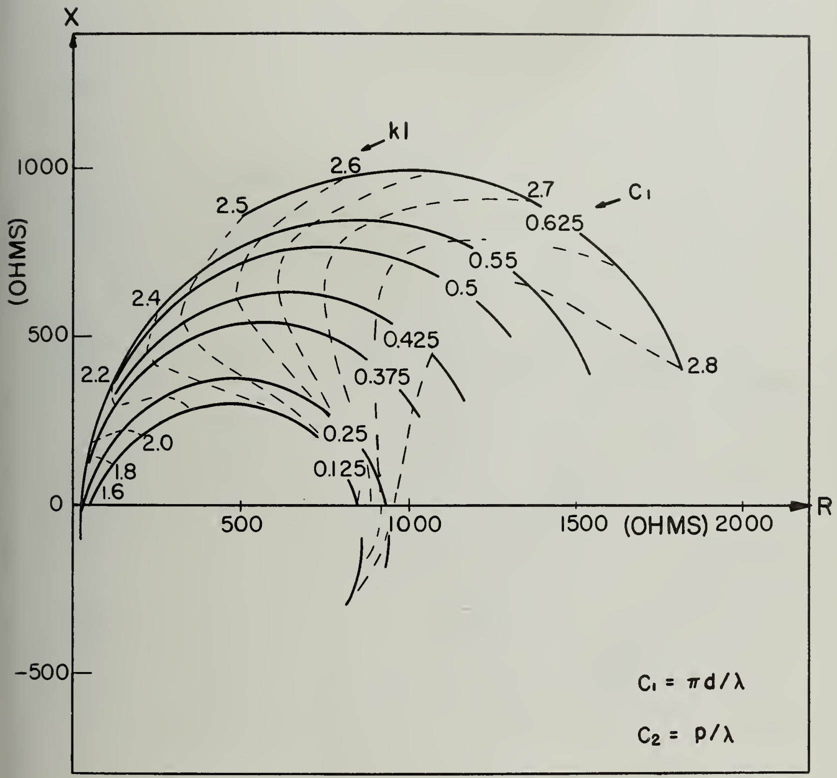

Figure 21b. The Input Impedance of Helical Antennas $C_2 = 0.25$

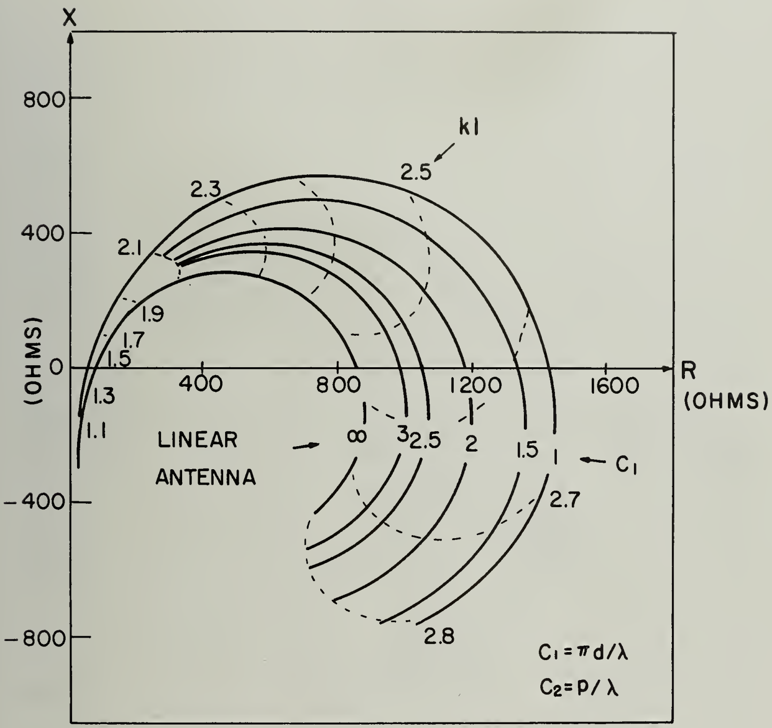

Figure 22a. The Input Impedances of Helical Antennas
$C_2 = 0.5$

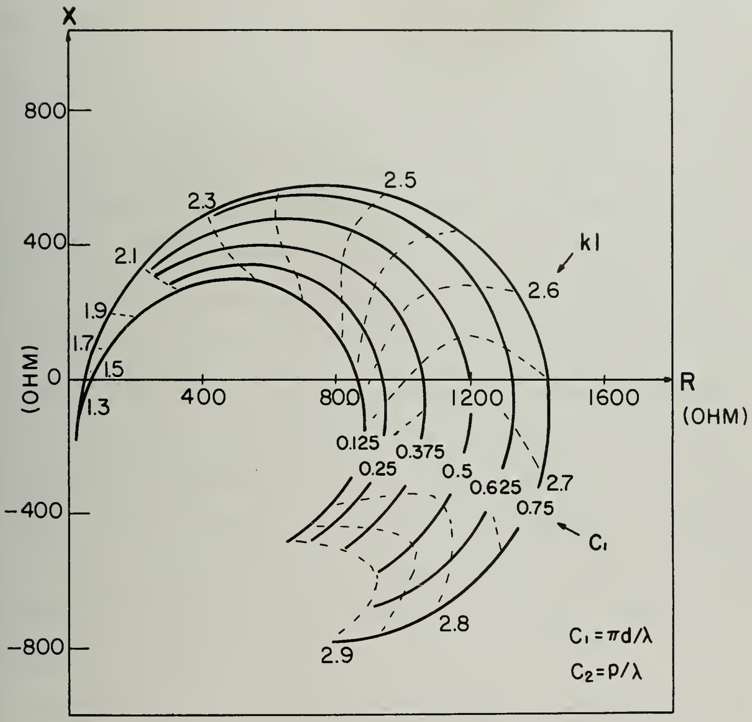

Figure 22b. The Input Impedances of Helical Antennas $C_2 = 0.5$

The characteristics of the input impedance as a function of the antenna arm length is exhibited by the equi-$k\ell$ contours. Generally speaking, when the antenna arm length is not long, say $k\ell < 2.1$, the characteristic of the equi-$k\ell$ contours behaves very much like that for the arc antenna; the reactance is almost constant while the resistance increases monotonically as the pitch is increased. For larger $k\ell$, the characteristic deviates both from that of the arc antenna and that of the cylindrical antenna. When the pitch of the helix is held constant and the radius of the helix is increased, the circular graph of the input impedance is first enlarged from that of the cylindrical antenna. It reaches a certain maximum and then starts to shrink to the input impedance of a cylindrical antenna again. This is because of the fact that helices of zero radius and infinite radius both become cylindrical antennas. For example, Figures 21a and 21b show the impedance for a constant pitch helical antenna for which $C_2 = 0.25$; in Figure 21a the circular graph becomes larger for smaller values of C_1 and it reaches the maximum at about $C_1 = 0.75$. For even smaller values of C_1 the circular graph shrinks and approaches to the impedance of the cylindrical antenna. Figures 22a and 22b give the impedance for $C_2 = 0.5$.

The convergence of the input impedance of helical antennas toward that of cylindrical antennas is shown in Figures 23 and 24. It is seen that there is a minimum in $(\mathcal{R})_{res}$ and a maximum in $(\mathcal{R})_{antires}$ for each given C_2. The locations of these extrema are shifted toward larger C_1 as we increase C_2.

(a) The location of minimums of $(\mathcal{R})_{res}$ are at

C_1	0.4	0.625	0.825	1.05	1.125	1.325
C_2	0.25	0.5	0.75	1	1.25	1.5
C_1/C_2	1.6	1.25	1.1	1.05	0.9	0.883

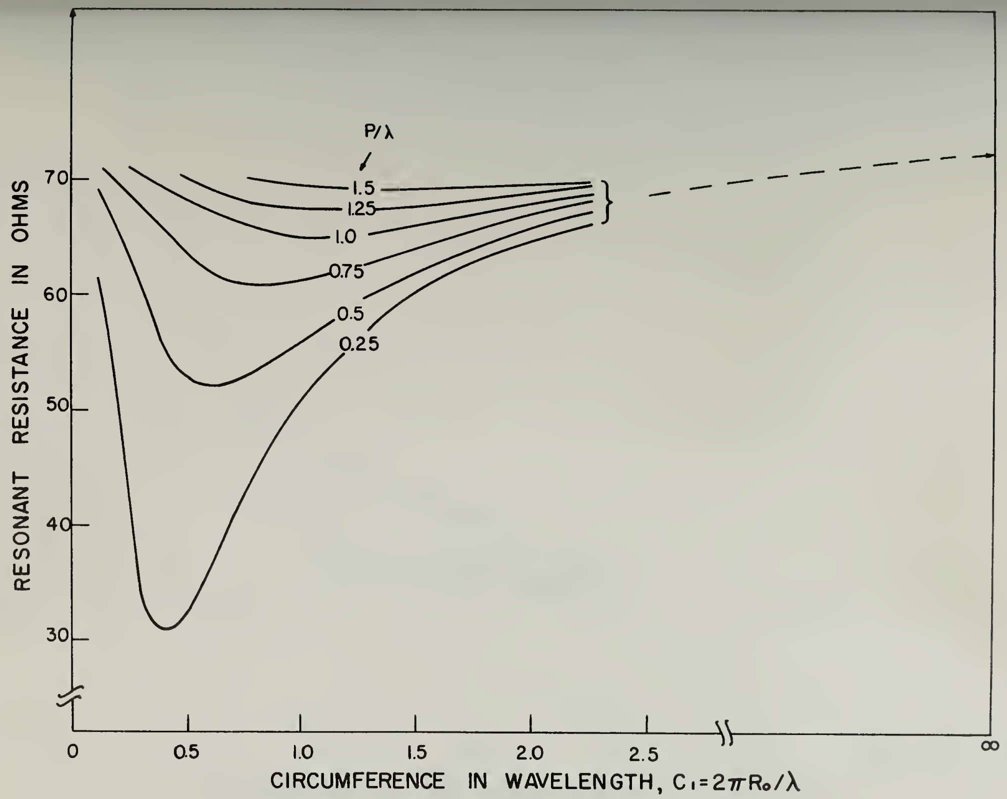

Figure 23. Resonant Resistance as a Function of Circumference in Wavelength

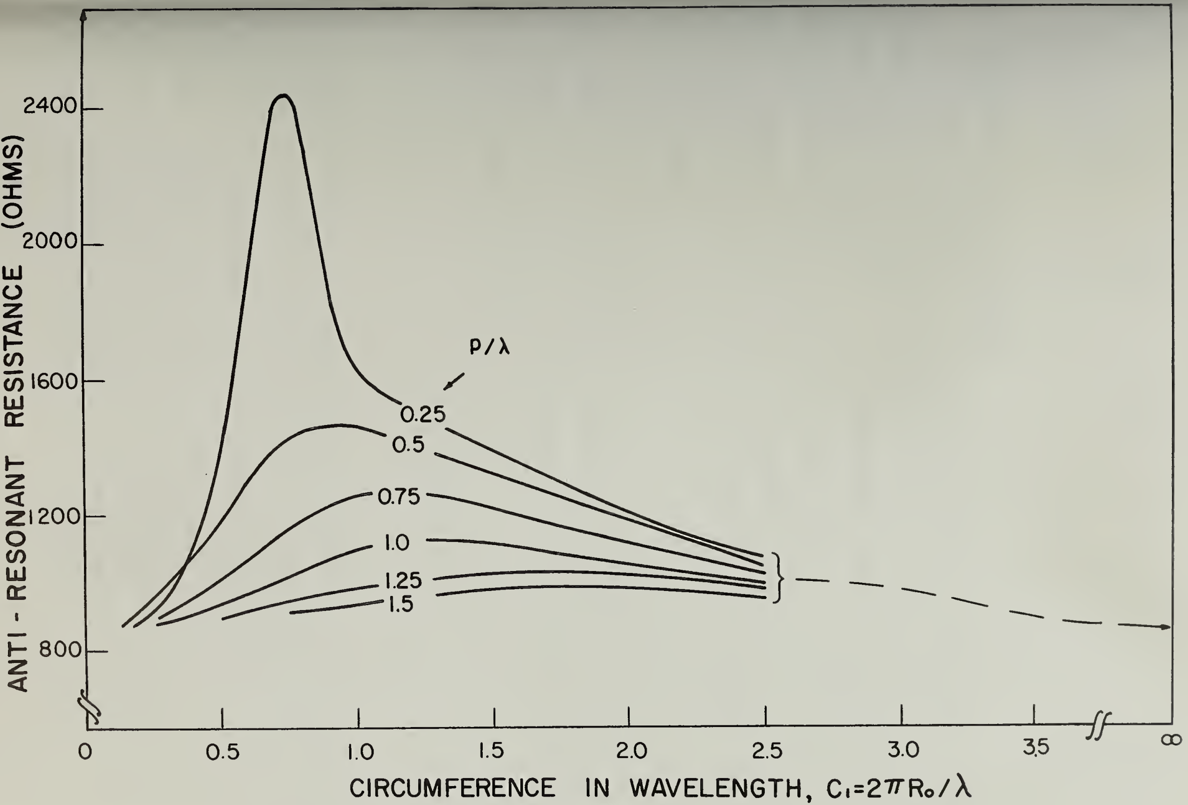

Figure 24. Antiresonant Resistance as a Function of Circumference in Wavelength

(b) The location of maximums of $(\mathcal{R})_{\text{antires}}$ are at

C_1	0.75	0.875	1.125	1.25	1.45	1.65
C_2	0.25	0.5	0.75	1	1.25	1.5
C_1/C_2	3	1.75	1.5	1.25	1.16	1.1

4.6 Equivalent Helical Antennas

Two helical antennas will be said to be equivalent with respect to the resonant resistance if they have the same resonant resistance. Similarly, they are equivalent with respect to the antiresonant resistance if they have the same antiresonant resistance. The contour lines of the resonant resistance are given in Figure 25 and that of the antiresonant resistance is in Figure 26. With these figures, one can readily determine the set of equivalent helical antennas as defined.

When the radius of the helix is large, the contour lines of the equivalent helices can be described very closely by the radius of the curvature of the helix, as expected. The normalized radius of curvature of the helix, as given by Equation (97) is

$$C_o = \frac{C_1^{\,2} + C_2^{\,2}}{C_1}$$

It is expected that for the relatively large values of C_1, the input impedance of a helical antenna with normalized radius of curvature C_o should approach that of an arc antenna with normalized radius C_1 when $C_o = C_1$ and $k\ell$ is not too large. Moreover, it is also natural to expect that for the relatively large values of C_1, two helical antennas of the same radius of curvature have the same input impedances. The Equation (97), with constant C_o, gives a set of

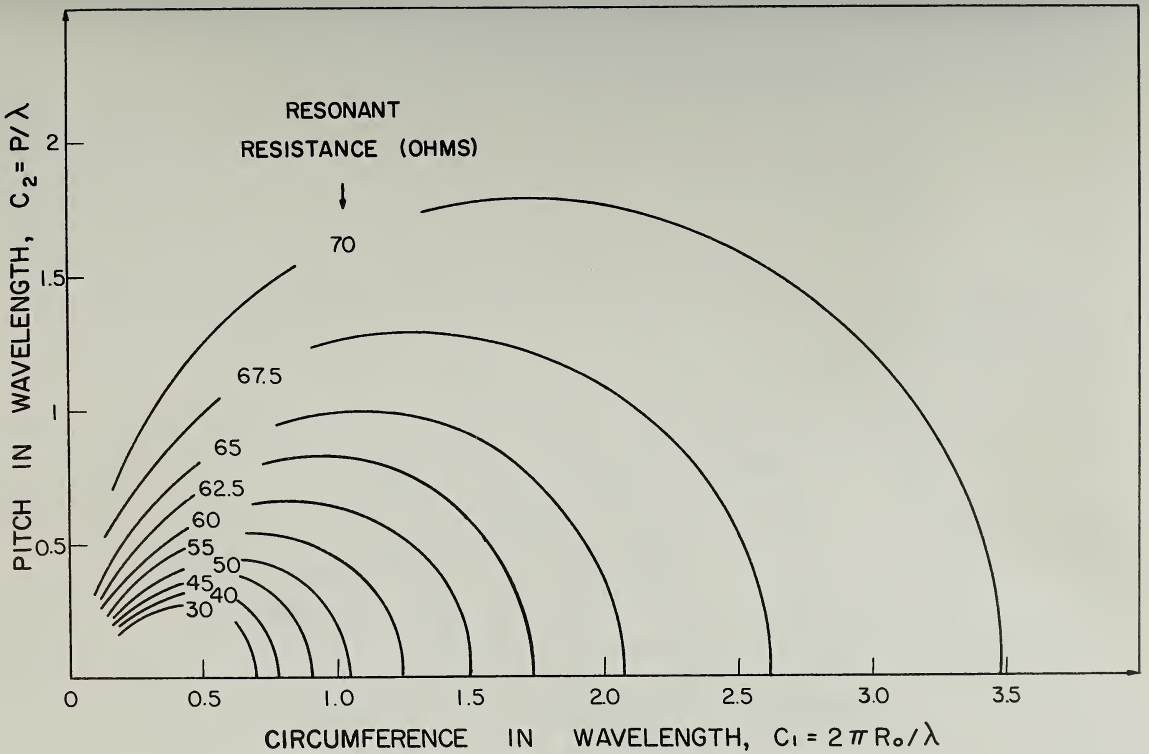

Figure 25. Equal Resonant Resistance Contours

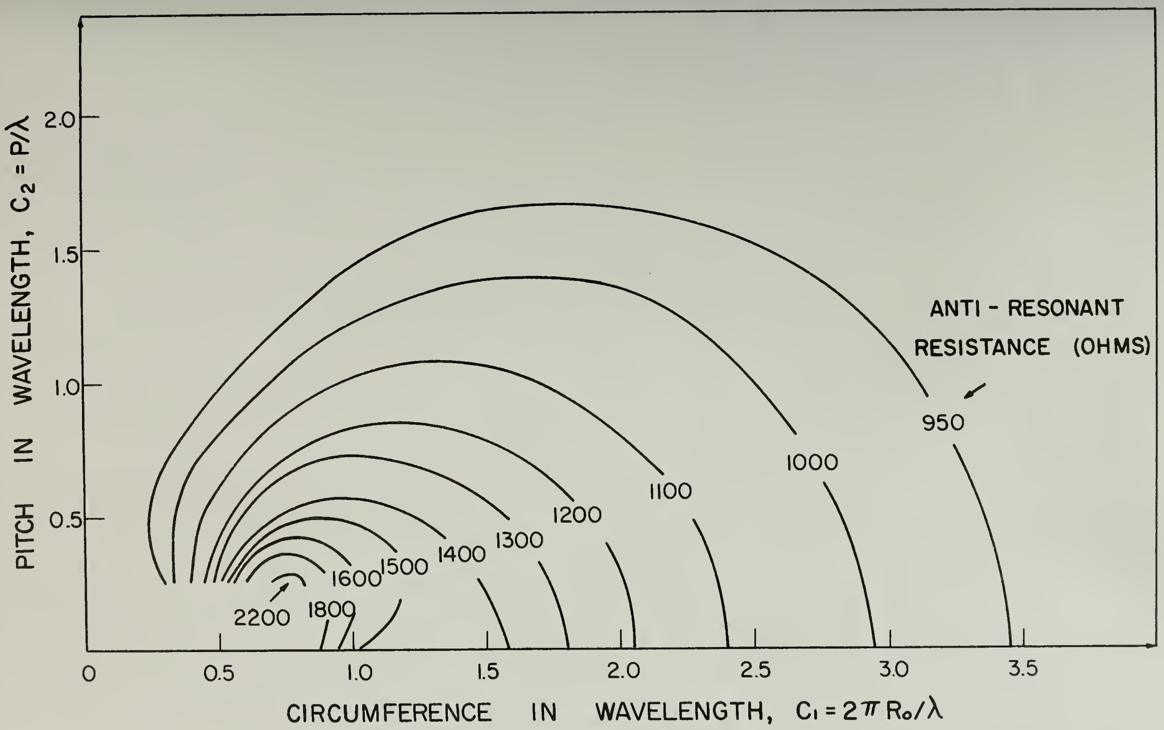

Figure 26. Equal Antiresonant Resistance Contours

circles with center at $\left(\frac{C_o}{2}, 0\right)$ and of radius $\frac{C_o}{2}$. Since it can be written as

$$\left(C_1 - \frac{C_o}{2}\right)^2 + C_2^{\,2} = \left(\frac{C_o}{2}\right)^2 \qquad (97')$$

Examining Figures 25 and 26, one finds that for large values of C_1 the contour lines of the input impedances of equivalent helical antennas are circles described by Equation (97'), that is to say, equivalent helical antennas are helical antennas with the same radius of curvature for the relatively large size of the helix. It is also seen from Figures 25 and 26 that when the size of the helix is relatively large, the equivalent helical antennas with respect to the resonant resistance are also equivalent helical antennas with respect to the antiresonant assistance.

5. SUMMARY OF THE RESULTS AND CONCLUSIONS

The integral equation formulation for the problem of thin wire antennas has been examined. The linearized integral equation has been derived by using the thin wire approximation, $ka \ll 1$, $\ell \gg a$. It was shown that there are three special types of wire antennas having a simplified kernel function, namely the difference kernel. They are the cylindrical antennas, the arc antennas and the helical antennas. The latter obviously includes the first two as special cases.

The input impedances of wire antennas were expressed in terms of a variational formula which involves the Hilbert's double integral. For the helical antennas, the set of double integrals in the impedance formula was reduced to single integrals.

The evaluation of the input impedances of the cylindrical antennas, the arc antennas and the helical antennas was performed for a large range of the parameters. Although the input impedances of the cylindrical antennas are now considered as a classical result, no results on the input impedance of the arc antennas and the helical antennas was available to date as far as the author is aware.

The input impedances for these antennas are shown in graphical form. For the arc antennas, the circular graph of the impedance enlarges as the curvature is increased, i.e. the resonant resistance increases while the antiresonant resistance decreases. This effect is similar to that of the cylindrical antennas as the thickness is decreased. The input impedances for the helical antennas are computed and the region where the input impedances of helical antennas approach that of cylindrical antennas is shown.

The shortening effect of the resonant wavelength and the antiresonant wavelength for the arc antennas are also investigated. It is interesting to note that the extreme value of the ratio of the resonant wavelength to the arc length measured by Englund is in good agreement with our computed result.

The equivalent helical antennas were defined and given. The contour lines are closely related to the set of circles for the constant radius of the curvature of helices.

BIBLIOGRAPHY

1. L. V. King, "On the Radiation Field of a Perfectly Conducting Base Insulated Antenna Over a Perfectly Conducting Plane Earth, and the Calculation of Radiation Resistance and Reactance", Phil. Trans. Roy. Soc. (Lond.) Ser. A. 236, 1937, pp. 381-422.

2. E. Hallen, "Theoretical Investigations into the Transmitting and Receiving Qualities of Antennas", Nova Acta (Uppsala) 11, 1938, No. 4.

3. R. King and D. Middleton, "The Cylindrical Antenna; Current and Impedance", Quart. Appl. Math. 3., 1946, pp. 302-335.

4. S. A. Schelkunoff, "Theory of Antennas of Arbitrary Size and Shape", IRE Proc. 29, 1941, pp. 493-521.

5. H. C. Pocklington, "Electrical Oscillation on Wires", Camb. Phil. Soc. Proc. 9, 1897, pp. 324-332.

6. J. E. Storer, "Theoretical Discussion of Circular Loops," TR212, Cruft Lab. Harvard U., 1955.

7. Olof Brundell, "Current and Potential Distribution on a Circular Loop Antenna", Trans. Royal Inst. of Tech., Stocholm, Sweden, No. 154, 1960.

8. J. E. Storer, "Variational Solution to the Problem of the Symmetrical Cylindrical Antenna", TR-101, Cruft Lab., Harvard U., 1950.

9. C. T. Tai, "A Variational Solution to the Problem of Cylindrical Antennas", TR-12, SRI Project No. 188, Stanford Research Institute, 1950.

10. C. R. Englund, "The Natural Period of Linear Conductors", B.S.T.J. Vol. 7-B, 1928, pp. 404-419.

11. S. A. Schelkunoff, "Advanced Antenna Theory", John Wiley & Sons, Inc. , New York, 1952, pp. 141 and 169.

12. C. T. Tai, "A New Interpretation of the Integral Equation Formulation of Cylindrical Antennas", IRE Trans. AP-3, 1955, pp.125.

13. R. W. P. King, "The Theory of Linear Antennas", Harvard University Press, Cambridge, Mass., 1956.

APPENDIX A

STRUCTURES WHICH GIVE CLOSED CYCLE TYPE KERNELS

Since the kernel function $\mathcal{K}_a$ is expressed in terms of the function $r_o(s,s')$, the Euclidean distance between two points in the curve. Therefore the structures giving rise to the closed cycle type kernel are those leading to the special property

$$r_o(s,s') = r_o\,(|s-s'|) \tag{A.1}$$

To show that the Euclidean distance between two points on a straignt line, a circular arc and a helix lead to the expression (A.1), we express an arbitrary curve by the following set of parametric equations

$$x = x(s) \tag{A.2}$$

$$y = y(s) \tag{A.3}$$

$$z = z(s) \tag{A.4}$$

The Euclidean distance between two points on the curve is thus

$$r(s,s') = \left\{[X(s) - X(s')]^2 + [y(s) - y(s')]^2 + [z(s) - z(s')]^2\right\}^{1/2} \tag{A.5}$$

which becomes the expression (A.1) in the following cases

(a) when x,y,z are linear functions of s. This describes a straight line.

(b) when the expression $[X(s) - X(s')]^2 + [y(s) - y(s')]^2$ has the property expressed in (A.1). A special set of transcendental functions satisfying this condition are

$$\begin{cases} x = \cos s \\ y = \sin s \end{cases} \quad \text{or} \quad \begin{cases} x = \sin s \\ y = \cos s \end{cases}$$

which describes a circle.

(c) The combination of cases (a) and (b) is a circular helix.

The fact that the Euclidean transformation includes only translation and/or rotation indicates that the circular helix is the most general structure, invariant under a one-dimensional Abelian group of congruent transformation.

The statement that a curve with the property

$$r_o(s,s') = r_o(|s-s'|)$$

is invariant under a one-parameter Abelian group of congruent transformation, will be elaborated as follows

(1) One Dimensional Case

When all points of the curve are on a straight line, it is trivial that they are invariant under the translation, which is a group transformation.

(2) Two Dimensional Case - plane curve

There exist three points of the curve forming a triangle. Any other points of the curve lie in the plane of the triangle. Let P_1, P_2 and P_3 be three points on the curve with arc lengths s_1, s_2 and s_3 respectively and consider three other points P_1', P_2' and P_3' with arc length $s_1' = s_1 + a$, $s_2' = s_2 + a$ and $s_3' = s_3 + a$. Then the triangle $(P_1P_2P_3)$ is congruent to the triangle $(P_1'P_2'P_3')$ and this defines a displacement T_a.

$$\triangle P_1P_2P_3 \longrightarrow \triangle P_1'P_2'P_3'$$

This displacement transforms the whole curve onto itself.

Proof: Take any other point P on the curve. The image of P under Ta is P'. Then the Euclidean distances from P' to P_1', P_2' and P_3' are equal to those from P to P_1, P_2 and P_3 respectively. Therefore P' is also on the curve. Furthermore, the displacement T_a is a rotation; it is a plane displacement and since case (1) is excluded it is not a translation.

The plane rotation with a fixed origin is a group transformation.

(3) Three Dimensional Case

There exist four points not coplanar, say P_1, P_2, P_3 and P_4 with arc lengths s_1, s_2, s_3 and s_4 respectively. Then similar reasoning to (2) gives points P_1', P_2', P_3' and P_4', with arc lengths $s_1' = s_1 + a$, $s_2' = s_2 + a$, $s_3' = s_3 + a$ and $s_4' = s_4 + a$ respectively, $P_1'P_2'P_3'P_4'$ forms a tetrahedron congruent to the first one and this defines a congruent transformation T_a

$$(P_1P_2P_3P_4) \longrightarrow (P_1'P_2'P_3'P_4')$$

which transforms the whole curve onto itself. This must be a helical transformation since (2) and (1) are excluded; the transformation T_a forms a group because $T_a\ T_b$ transforms P(s) to P'(s + a + b) which is the same as the transformation T_{a+b}.

These group transformations are Abelian, since in each case we have $T_aT_b = T_bT_a$.

APPENDIX B

TRANSFORMATIONS OF SOME DOUBLE INTEGRALS

Double integrals of the type

$$I = \int_0^{\ell} \int_0^{\ell} F_1(s + s')\, F_2(s - s')\, ds'\, ds \tag{B.1}$$

can be transformed into single integrals by the transformation

$$\begin{aligned} s + s' &= u \\ s - s' &= v \end{aligned} \tag{B.2}$$

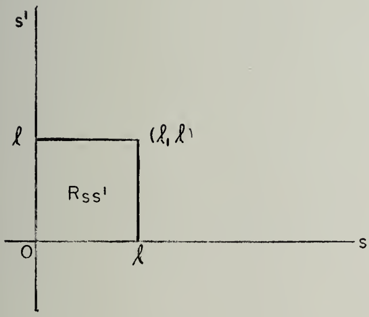

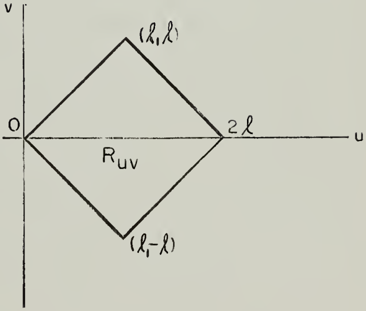

The Jacobian of the transformation is

$$J = \left| \frac{\partial(s, s')}{\partial(u, v)} \right| = \frac{1}{2} \tag{B.3}$$

and in terms of u,v, the given double integral is

$$I = \iint_{Ruv} F_1(u)\, F_2(v)\, \frac{1}{2}\, du\, dv \tag{B.4}$$

which can be integrated into single integrals in the following ways

$$I = \int_o^{\ell} \frac{F_2(v) + F_2(-v)}{2} \left(\int_v^{2\ell - v} F_1(u)\, du \right) dv \tag{B.5}$$

$$I = \int_o^{\ell} F_1(u) \left(\int_{-u}^{u} \frac{F_2(v)}{2}\, dv \right) du + \int_{\ell}^{2\ell} F_1(u) \left(\int_{u-2\ell}^{2\ell - u} \frac{F_2(v)}{2}\, dv \right) du \tag{B.6}$$

Applying these formulas, a list of double integrals which are useful to the derivation of input impedance formulas are given below.

1. $$\iint\limits_{u\;v} \sin u \; G(u) \; \frac{1}{2} \; du \; dv = \int_{0}^{\ell} u \sin u \; G(u) \; du + \int_{\ell}^{2\ell} (2\ell-u) \sin u \; G(u) \; du$$

2. $$\iint\limits_{u\;v} \cos u \; G(u) \; \frac{1}{2} \; du \; dv = \int_{0}^{\ell} u \cos u \; G(u) \; du + \int_{\ell}^{2\ell} (2\ell-u) \cos u \; G(u) \; du$$

3. $$\iint\limits_{u\;v} \sin u \; G(u) \; \frac{1}{2} \; du \; dv = \int_{0}^{\ell} [\cos v - \cos (2\ell-v)] \; G(v) \; dv$$

4. $$\iint\limits_{uv} \cos u \; G(v) \; \frac{1}{2} \; du \; dv = \int_{0}^{\ell} [\sin (2\ell-v) - \sin v] \; G(v) \; dv$$

5. $$\iint\limits_{u\;v} \sin v \; G(v) \; \frac{1}{2} \; du \; dv = 0$$

6. $$\iint\limits_{u\;v} \cos v \; G(v) \; \frac{1}{2} \; du \; dv = \int_{0}^{\ell} 2(\ell-u) \cos v \; G(v) \; dv$$

7. $$\iint\limits_{u\;v} \sin v \; G(u) \; \frac{1}{2} \; du \; dv = 0$$

8. $$\iint\limits_{u\;v} \cos v \; G(u) \; \frac{1}{2} \; du \; dv = \int_{0}^{\ell} \sin u \; G(u) \; du + \int_{\ell}^{2\ell} \sin (2\ell-u) \; G(u) \; du$$

9. $$\iint\limits_{u\;v} u \sin u \; G(u) \; \frac{1}{2} \; du \; dv = \int_{0}^{\ell} u^{2} \sin u \; G(u) \; du + \int_{\ell}^{2\ell} (2\ell-u) \; u \sin u \; G(u) \; du$$

0. $$\iint\limits_{u\;v} u \cos u \; G(u) \; \frac{1}{2} \; du \; dv = \int_{0}^{\ell} u^{2} \cos u \; G(u) \; du + \int_{\ell}^{2\ell} (2\ell-u) \; u \cos u \; G(u) \; du$$

11. $$\int_u\int_v u \sin u\, G(v)\, \frac{1}{2}\, du\, dv = \int_0^{\ell} [\sin (2\ell-v)-(2\ell-v) \cos(2\ell-v)-\sin v+v \cos v]G(v)dv$$

12. $$\int_u\int_v u \cos u\, G(v)\, \frac{1}{2}\, dudv = \int_0^{\ell} [\cos(2\ell-v)+(2\ell-v)\sin(2\ell-v)-\cos v-v \sin v]G(v)\, dv$$

13. $$\int_u\int_v u \sin v\, G(v)\, \frac{1}{2}\, du\, dv = 0$$

14. $$\int_u\int_v u \cos v\, G(v)\, \frac{1}{2}\, du\, dv = \int_0^{\ell} 2\ell(\ell-v) \cos v\, G(v)\, dv$$

5. $$\int_u\int_v u \sin v\, G(u)\, \frac{1}{2}\, du\, dv = 0$$

6. $$\int_u\int_v u \cos v\, G(u)\, \frac{1}{2}\, du\, dv = \int_0^{\ell} u \sin u\, G(u)\, du + \int_{\ell}^{2\ell} u \sin (2\ell-u)\, G(u)\, du$$

7. $$\int_u\int_v v \sin u\, G(u)\, \frac{1}{2}\, du\, dv = 0$$

8. $$\int_u\int_v v \cos u\, G(u)\, \frac{1}{2}\, du\, dv = 0$$

9. $$\int_u\int_v v \sin u\, G(v)\, \frac{1}{2}\, du\, dv = 0$$

0. $$\int_u\int_v v \cos u\, G(v)\, \frac{1}{2}\, du\, dv = 0$$

21. $$\iint_{u\,v} v \sin v \, G(v) \, \frac{1}{2} \, du \, dv = \int_{0}^{\ell} 2(\ell - v) \, v \sin v \, G(v) \, dv$$

22. $$\iint_{u\,v} v \cos v \, G(v) \, \frac{1}{2} \, du \, dv = 0$$

23. $$\iint_{u\,v} v \sin v \, G(u) \, \frac{1}{2} \, du \, dv = \int_{0}^{\ell} [\sin u - u \cos u] G(u) du + \int_{\ell}^{2\ell} [\sin(2\ell - u) - (2\ell - u) \cos(2\ell - u)] \, G(u) \, du$$

24. $$\iint_{u\,v} v \cos v \, G(u) \, \frac{1}{2} \, du \, dv = 0$$

25. $$\iint_{u\,v} u^{2} \sin u \, G(u) \, \frac{1}{2} \, du \, dv = \int_{0}^{\ell} u^{3} \sin u \, G(u) \, du + \int_{\ell}^{2\ell} u^{2} (2\ell - u) \sin u \, G(u) \, du$$

26. $$\iint_{u\,v} u^{2} \cos u \, G(u) \, \frac{1}{2} \, du \, dv = \int_{0}^{\ell} u^{3} \cos u \, G(u) du + \int_{\ell}^{2\ell} u^{2} (2\ell - u) \cos u \, G(u) \, du$$

27. $$\iint_{u\,v} u^{2} \sin u \, G(v) \, \frac{1}{2} \, du \, dv = \int_{0}^{\ell} [2(2\ell - v) \sin(2\ell - v) - (4\ell^{2} - 4\ell v + v^{2} - 2) \cos (2\ell - v) - 2v \sin v + (v^{2} - 2) \cos v] \, G(v) \, dv$$

28. $$\iint_{u\,v} u^{2} \cos u \, G(v) \, \frac{1}{2} \, du \, dv = \int_{0}^{\ell} [2(2\ell - v) \cos(2\ell - v) + (4\ell^{2} - 4\ell v + v^{2} - 2) \sin(2\ell - v) - 2v \cos v - (v^{2} - 2) \sin v] \, G(v) \, dv$$

29. $$\iint_{u\,v} u^2 \sin v\; G(v)\, \frac{1}{2}\, du\, dv = 0$$

30. $$\iint_{u\,v} u^2 \cos v\; G(v)\, \frac{1}{2}\, du\, dv = \int_0^{\ell} \frac{1}{3}[8\ell^3 - 12\ell^2 v + 6\ell v^2 - 2v^3] \cos v\; G(v)\, dv$$

31. $$\iint_{u\,v} u^2 \sin v\; G(u)\, \frac{1}{2}\, du\, dv = 0$$

32. $$\iint_{u\,v} u^2 \cos v\; G(u)\, \frac{1}{2}\, du\, dv = \int_0^{\ell} u^2 \sin u\; G(u)\, du + \int_{\ell}^{2\ell} u^2 \sin(2\ell - u) G(u)\, du$$

33. $$\iint_{u\,v} v^2 \sin u\; G(u)\, \frac{1}{2}\, du\, dv = \int_0^{\ell} \frac{1}{3}\, u^3 \sin u\; G(u)\, du + \int_{\ell}^{2\ell} \frac{1}{3}\, (2\ell - u)^3 \sin u\; G(u) du$$

34. $$\iint_{u\,v} v^2 \cos u\; G(u)\, \frac{1}{2}\, du\, dv = \int_0^{\ell} \frac{1}{3} u^3 \cos u\; G(u) du + \int_{\ell}^{2\ell} \frac{1}{3}(2\ell - u)^3 \cos u\; G(u)\, du$$

35. $$\iint_{u\,v} v^2 \sin u\; G(v)\, \frac{1}{2}\, du\, dv = \int_0^{\ell} v^2 [\cos v - \cos\,(2\ell - v)]\, G(v)\, dv$$

36. $$\iint_{u\,v} v^2 \cos u\; G(v)\, \frac{1}{2}\, du\, dv = \int_0^{\ell} v^2\, [\sin\,(2\ell - v) - \sin\, v]\, G(v)\, dv$$

37. $$\iint_{u\,v} v^2 \sin v\; G(v)\, \frac{1}{2}\, du\, dv = 0$$

38. $$\iint_{u\,v} v^2 \cos v\, G(v)\, \frac{1}{2}\, du\, dv = \int_o^{\ell} 2v^2(\ell - v) \cos v\, G(v)\, dv$$

39. $$\iint_{u\,v} v^2 \sin v\, G(u)\, \frac{1}{2}\, du\, dv = 0$$

40. $$\iint_{u\,v} v^2 \cos v\, G(u)\, \frac{1}{2}\, du\, dv = \int_1^{\ell} [2u \cos u + (u^2 - 2) \sin u]\, G(u)\, du$$

$$+ \int_{\ell}^{2\ell} [2(2\ell - u) \cos (2\ell - u) + (4\ell^2 - 4\ell u + u^2 - 2) \sin (2\ell - u)]$$

$$G(u)\, du$$

APPENDIX C

COMPUTATIONAL PROCEDURES

The numerical computations were carried out on ILLIAC, the digital computer of the University of Illinois. The computation involved two parts.

(a) The integration of the set of integrals ν_1, ν_2, and ν_3. They can be written as

$$\nu_i = \left[\int_0^L F_{i1}(x) \frac{\cos \bar{r}(x)}{\bar{r}(x)} dx + \int_L^{2L} F_{i2}(x) \frac{\cos \bar{r}(x)}{\bar{r}(x)} dx \right]$$

$$+ j \left[\int_0^L F_{i1}(x) \frac{\sin \bar{r}(x)}{\bar{r}(x)} dx + \int_L^{2L} F_{i2}(x) \frac{\sin \bar{r}(x)}{\bar{r}(x)} dx \right]$$

$$i = 1,2,3.$$

where F_{i1}'s and F_{i2}'s are given by the Equations (86) through (91) and $\bar{r}(x)$ is given by Equation (93) for the helical antennas and Equation (95) for the arc antennas.

The integration was performed by using Simpson's rule. The set of functions F_{ij}'s were first evaluated by the auxiliary routines; the results then entered the integration routine with the assigned number of intervals for the integration. This number was determined by the convergence of the result, which will be explained later.

(b) The algebraic operations for the impedance formula.

After the set of integrals ν_1, ν_2 and ν_3 are evaluated, the set of complex numbers

$$\nu_i = \sigma_i + j \tau_i \qquad i = 1,2,3$$

entered the first order impedance formula as follows

$$Z_{in}^{(1)} = j30 \frac{\nu_1 \nu_3 - \nu_2^2}{(\sin^2 L)\,\nu_3 - (L \sin 2L)\,\nu_2 + (L^2 \cos^2 L)\,\nu_1} = \frac{\alpha + j\beta}{\gamma + j\delta}$$

$$= \frac{\alpha\gamma + \beta\delta}{\gamma^2 + \delta^2} + j\,\frac{\beta\gamma - \alpha\delta}{\gamma^2 + \delta^2}$$

where

$$\alpha = -30[\tau_1\sigma_3 + \sigma_1\tau_3 - 2\sigma_2\tau_2]$$

$$\beta = 30[\sigma_1\sigma_3 - \tau_1\tau_3 - \sigma_2^2 + \tau_2^2]$$

$$\gamma = \sigma_3 \sin^2 L - \sigma_2 L \sin 2L + \sigma_1 L^2 \cos^2 L$$

$$\delta = \tau_3 \sin^2 L - \tau_2 L \sin 2L + \tau_1 L^2 \cos^2 L$$

The computer program was prepared for computing the impedance of the helical antennas for a given set of parameters C_1, C_2, L and Ω. These parameters are defined as

$$C_1 = kR_o = 2\pi R_o/\lambda$$

$$C_2 = kb = p/\lambda$$

$$L = k\ell$$

$$\Omega = 2\,\ell n \frac{2\ell}{a}$$

where

R_o is the radius of the helix

ℓ is the half length of the antenna

a is the thickness of the antenna wire

and

$$b = p/2\pi$$

where

p is the pitch of the helix

The arc antennas and the cylindrical antennas are special cases of the helical antennas. For the arc antennas

$$C_2 = 0$$

and for the cylindrical antennas

$$C_1 = \infty, \qquad C_2 = 0$$

The program was coded in such a way that it could compute automatically the impedances for several values of L. The published results of the input impedances for cylindrical antennas were used as guides in checking the computation program.

Since for those integrals involving Cos $\overline{r}(x)/\overline{r}(x)$, the integrand gives a large value when x = 0, the integral

$$\int_o^L F_{il}(x) \frac{\cos \overline{r}(x)}{\overline{r}(x)} \, dx$$

was split into

$$\int_o^{\Delta} F_{il}(x) \frac{\cos \overline{r}(x)}{\overline{r}(x)} \, dx + \int_{\Delta}^{L} F_{il}(x) \frac{\cos \overline{r}(x)}{\overline{r}(x)} \, dx$$

where the value Δ together with the number of points in the Simpson's integration rule were determined by the stability of the results. A fixed number $n = 20$ for the integration interval was used to determine the stable value for Δ. The computation results for a series of integrals indicate that $\Delta = 0.25$ was an optimum value. The value $\Delta = 0.25$ was then used in the splitting of the above mentioned integrals. To determine the number of the integration intervals the integrals were evaluated with a set of different number n. After analyzing these results, we chose the value $n = 30$. For this combination of values of Δ and n, the impedance for the cylindrical antennas were compared with that obtained by Tai, for $\Omega = 10$ and $\Omega = 15$. The comparison showed that in the range $L < 6$, the difference between these two results is 3 % at the most.

AF33(657)-8460

DISTRIBUTION LIST

One copy each unless otherwise indicated

Armed Services Technical Information Agency
Attn: TIP-DR
Arlington Hall Station
Arlington 12, Virginia (10 copies)

Aeronuatical Systems Division
Attn: (ASRNRE-4)
Wright-Patterson Air Force Base
Ohio (3 copies)

Aeronautical Systems Division
Attn: ASDSED, Mr. Mulligan
Wright-Patterson Air Force Base
Ohio

Aeronautical Systems Division
Attn: AFCIN-4B1A
Wright-Patterson Air Force Base
Ohio

Air Force Cambridge Research Laboratory
Attn: CRRD
Laurence G. Hanscom Field
Bedford, Massachusetts

Commander
Air Force Missile Test Center
Patrick Air Force Base
Florida

Commander
Air Force Missile Development Center
Attn: Technical Library
Holloman Air Force Base
New Mexico

Air Force Ballistic Missile Division
Attn: Technical Library, Air Force Unit Post Office
Los Angeles, California

Director
Ballistics Research Laboratory
Attn: Ballistics Measurement Lab.
Aberdeen Proving Ground, Maryland

National Aeronautics & Space Adm.
Attn: Librarian
Langley Field, Virginia

Rome Air Development Center
Attn: RCLTM
Griffiss Air Force Base
New York

Research & Development Command
Hq. USAF (ARDRD-RE)
Washington 25, D. C.

Office of Chief Signal Officer
Engineering & Technical Division
Attn: SIGNET-5
Washington 25, D. C.

Commander
U. S. Army White Sands Signal Agency
Attn: SIGWS-FC-02
White Sands, New Mexico

Director
Surveillance Department
Evans Area
Attn: Technical Document Center
Belman, New Jersey

Commander
U. S. Naval Air Test Center
Attn: WST-54, Antenna Section
Patuxent River, Maryland

Material Laboratory, Code 932
New York Naval Shipyard
Brooklyn 1, New York

Commanding Officer
Diamond Ordnance Fuse Laboratories
Attn: 240
Washington 25, D. C.

Director
U. S. Navy Electronics Laboratory
Attn: Library
San Diego 52, California

Adams-Russell Company
200 Sixth Street
Attn: Library (Antenna Section)
Cambridge, Massachusetts

Aero Geo Astro
Attn: Security Officer
1200 Duke Street
Alexandria, Virginia

NASA Goddard Space Flight Center
Attn: Antenna Section, Code 523
Creenbelt, Maryland

Airborne Instruments Labs., Inc.
Attn: Librarian (Antenna Section)
Walt Whitman Road
Melville, L. I., New York

American Electronic Labs
Box 552 (Antenna Section)
Lansdale, Pennsylvania

Andrew Alfred Consulting Engineers
Attn: Librarian (Antenna Section)
299 Atlantic Ave.
Boston 10, Massachusetts

Ampheol-Borg Electronic Corporation
Attn: Librarian (Antenna Section)
2801 S. 25th Avenue
Broadview, Illinois

Bell Aircraft Corporation
Attn: Technical Library
(Antenna Section)
Buffalo 5, New York

Bendix Radio Division of
Bendix Aviation Corporation
Attn: Technical Library
(For Dept. 462-4)
Baltimore 4, Maryland

Boeing Airplane Company
Aero Space Division
Attn: Technical Library
M/F Antenna & Radomes Unit
Seattle, Washington

Boeing Airplane Company
Attn: Technical Library
M/F Antenna Systems Staff Unit
Wichita, Kansas

Chance Vought Aircraft Inc.
THRU: BU AER Representative
Attn: Technical Library
M/F Antenna Section
P. O. Box 5907
Ballas 22, Texas

Collins Radio Company
Attn: Technical Library (Antenna Section)
Dallas, Texas

Convair
Ft. Worth Division
Attn: Technical Library (Antenna Section)
Grants Lane
Fort Worth, Texas

Convair
Attn: Technical Library (Antenna Section)
P. O. Box 1050
San Diego 12, California

Dalmo Victor Company
Attn: Technical Library (Antenna Section)
1515 Industrial Way
Belmont, California

Dorne & Margolin, Inc.
Attn: Technical Library (Antenna Section)
30 Sylvester Street
Westbury, L. I., New York

Dynatronics Inc.
Attn: Technical Library (Antenna Section)
Orlando, Florida

Electronic Communications, Inc.
Research Division
Attn: Technical Library
1830 York Road
Timonium, Maryland

Fairchild Engine & Airplane Corporation
Fairchild Aircraft & Missiles Division
Attn: Technical Library (Antenna
Section)
Hagerstown 10, Maryland

Georgia Institute of Technology
Engineering Experiment Station
Attn: Technical Library
M/F Electronics Division
Atlanta 13, Georgia

General Electric Company
Electronics Laboratory
Attn: Technical Library
Electronics Park
Syracuse, New York

General Electronic Labs., Inc.
Attn: Technical Library (Antenna
Section)
18 Ames Street
Cambridge 42, Massachusetts

General Precision Lab., Division of
General Precision Inc.
Attn: Technical Library (Antenna
Section)
63 Bedford Road
Pleasantville, New York

Goodyear Aircraft Corporation
Attn: Technical Library
M/F Dept. 474
1210 Massilon Road
Akron 15, Ohio

Granger Associates
Attn: Technical Library (Antenna
Section)
974 Commercial Street
Palo Alto, California

Grumman Aircraft Engineering Corp.
Attn: Technical Library
M/F Avionics Engineering
Bethpage, New York

The Hallicrafters Company
Attn: Technical Library (Antenna
Section)
4401 W. Fifth Avenue
Chicago 24, Illinois

Hoffman Laboratories Inc.
Attn: Technical Library (Antenna
Section)
Los Angeles 7, California

John Hopkins University
Applied Physics Laboratory
8621 Georgia Avenue
Silver Springs, Maryland

Hughes Aircraft Corporation
Attn: Technical Library (Antenna
Section)
Florence & Teal Street
Culver City, California

ITT Laboratories
Attn: Technical Library (Antenna
Section)
500 Washington Avenue
Nutley 10, New Jersey

U. S. Naval Ordnance Lab.
Attn: Technical Library
Corona, California

Lincoln Laboratories
Massachusetts Institute of Technology
Attn: Document Room
P. O. Box 73
Lexington 73, Massachusetts

Litton Industries
Attn: Technical Library (Antenna
Section)
4900 Calvert Road
College Park, Maryland

Lockheed Missile & Space Division
Attn: Technical Library (M/F Dept-58-40, Plant 1, Bldg. 130)
Sunnyvale, California

The Martin Company
Attn: Technical Library (Antenna Section)
P. O. Box 179
Denver 1, Colorado

The Martin Company
Attn: Technical Library (Antenna Section)
Baltimore 3, Maryland

The Martin Company
Attn: Technical Library (M/F Microwave Laboratory)
Box 5837
Orlando, Florida

W. L. Maxson Corporation
Attn: Technical Library (Antenna Section)
460 West 34th Street
New York 1, New York

McDonnell Aircraft Corporation
Attn: Technical Library (Antenna Section)
Box 516
St. Louis 66, Missouri

Melpar, Inc.
Attn: Technical Library (Antenna Section)
3000 Arlington Blvd.
Falls Church, Virginia

University of Michigan
Radiation Laboratory
Willow Run
201 Catherine Street
Ann Arbor, Michigan

Mitre Corporation
Attn: Technical Library (M/F Electronic Warfare Dept. D-21)
Middlesex Turnpike
Bedford, Massachusetts

North American Aviation Inc.
Attn: Technical Library (M/F Engineering Dept.)
4300 E. Fifth Avenue
Columbus 16, Ohio

North American Aviation Inc.
Attn: Technical Library (M/F Dept. 56)
International Airport
Los Angeles, California

Northrop Corporation
NORAIR Division
1001 East Broadway
Attn: Technical Information (3924-3)
Hawthorne, California

Ohio State University Research Foundation
Attn: Technical Library (M/F Antenna Laboratory)
1314 Kinnear Road
Columbus 12, Ohio

Philco Corporation
Government & Industrial Division
Attn: Technical Library (M/F Antenna Section)
4700 Wissachickon Avenue
Philadelphia 44, Pennsylvania

Westinghouse Electric Corporation
Air Arms Division
Attn: Librarian (Antenna Lab)
P. O. Box 746
Baltimore 3, Maryland

Wheeler Laboratories
Attn: Librarian (Antenna Lab)
Box 561
Smithtown, New York

Electrical Engineering Research Laboratory
University of Texas
Box 8026, Univ. Station
Austin, Texas

University of Michigan Research Institute
Electronic Defense Group
Attn: Dr. J. A. M. Lyons
Ann Arbor, Michigan

ıdio Corporation of America
CA Laboratories Division
ttn: Technical Library
(M/F Antenna Section)
rinceton, New Jersey

ıdiation, Inc.
ttn: Technical Library (M/F)
Antenna Section
rawer 37
elbourne, Florida

ıdioplane Company
tn: Librarian (M/F Aerospace Lab)
)00 Woodly Avenue
ın Nuys, California

ımo-Wooldridge Corporation
tn: Librarian (Antenna Lab)
noga Park, California

ınd Corporation
tn: Librarian (Antenna Lab)
700 Main Street
ınta Monica, California

ıntec Corporation
tn: Librarian (Antenna Lab)
3999 Ventura Blvd.
ılabasas, California

ıytheon Electronics Corporation
tn: Librarian (Antenna Lab)
)89 Washington Street
ewton, Massachusetts

epublic Aviation Corporation
pplied Research & Development
Division
tn: Librarian (Antenna Lab)
ırmingdale, New York

ınders Associates
tn: Librarian (Antenna Lab)
Canal Street
ıshua, New Hampshire

ꞁuthwest Research Institute
tn: Librarian (Antenna Lab)
00 Culebra Road
ın Antonio, Texas

H. R. B. Singer Corporation
Attn: Librarian (Antenna Lab)
State College, Pennsylvania

Sperry Microwave Electronics Company
Attn: Librarian (Antenna Lab)
P. O. Box 1828
Clearwater, Florida

Sperry Gyroscope Company
Attn: Librarian (Antenna Lab)
Great Neck, L. I., New York

Stanford Electronic Laboratory
Attn: Librarian (Antenna Lab)
Stanford, California

Stanford Research Institute
Attn: Librarian (Antenna Lab)
Menlo Park, California

Sylvania Electronic System
Attn: Librarian (M/F Antenna &
Microwave Lab)
100 First Street
Waltham 54, Massachusetts

Sylvania Electronic System
Attn: Librarian (Antenna Lab)
P. O. Box 188
Mountain View, California

Technical Research Group
Attn: Librarian (Antenna Section)
2 Aerial Way
Syosset, New York

Ling Temco Aircraft Corporation
Temco Aircraft Division
Attn: Librarian (Antenna Lab)
Garland, Texas

Texas Instruments, Inc.
Attn: Librarian (Antenna Lab)
6000 Lemmon Ave.
Dallas 9, Texas

A. S. Thomas, Inc.
Attn: Librarian (Antenna Lab)
355 Providence Highway
Westwood, Massachusetts

New Mexico State University
Head Antenna Department
Physical Science Laboratory
University Park, New Mexico

Bell Telephone Laboratories, Inc.
Whippany Laboratory
Whippany, New Jersey
Attn: Technical Reports Librarian
Room 2A-165

Robert C. Hansen
Aerospace Corporation
Box 95085
Los Angeles 45, California

Dr. Richard C. Becker
10829 Berkshire
Westchester, Illinois

Dr. Harry Letaw, Jr.
Raytheon Company
Surface Radar and Navigation
Operations
State Road West
Wayland, Massachusetts

Dr. Frank Fu Fang
IBM Research Laboratory
Poughkeepsie, New York

Mr. Dwight Isbell
1422 11th West
Seattle 99, Washington

Dr. Robert L. Carrel
Collins Radio Corporation
Antenna Section
Dallas, Texas

Dr. A. K. Chatterjee
Vice Principal & Head of the Department
of Research
Birla Institute of Technology
P. O. Mesra
District-Ranchi (Bihar) India

Aeronautical Systems Division
Attn: ASAD - Library
Wright-Patterson Air Force Base
Ohio

National Bureau of Standards
Department of Commerce
Attn: Dr. A. G. McNish
Washington 25, D. C.

ANTENNA LABORATORY
TECHNICAL REPORTS AND MEMORANDA ISSUED

ntract AF33(616)-310

ynthesis of Aperture Antennas," Technical Report No. 1, C.T.A. Johnk, tober, 1954.*

Synthesis Method for Broad-band Antenna Impedance Matching Networks," chnical Report No. 2, Nicholas Yaru, 1 February 1955.* AD 61049.

he Assymmetrically Excited Spherical Antenna," Technical Report No. 3, bert C. Hansen, 30 April 1955.*

nalysis of an Airborne Homing System," Technical Report No. 4, Paul E. yes, 1 June 1955 (CONFIDENTIAL).

oupling of Antenna Elements to a Circular Surface Waveguide," Technical port No. 5, H. E. King and R. H. DuHamel, 30 June 1955.*

xially Excited Surface Wave Antennas," Technical Report No. 7, D. E. Royal, October 1955.*

oming Antennas for the F-86F Aircraft (450-2500 mc)," Technical Report No. 8, E. Mayes, R. F. Hyneman, and R. C. Becker, 20 February 1957, (CONFIDENTIAL).

round Screen Pattern Range," Technical Memorandum No. 1, Roger R. Trapp, July 1955.*

ntract AF33(616)-3220

ffective Permeability of Spheroidal Shells," Technical Report No. 9, E. J. ott and R. H. DuHamel, 16 April 1956.

n Analytical Study of Spaced Loop ADF Antenna Systems," Technical Report . 10, D. G. Berry and J. B. Kreer, 10 May 1956. AD 98615

Technique for Controlling the Radiation from Dielectric Rod Waveguides," chnical Report No. 11, J. W. Duncan and R. H. DuHamel, 15 July 1956.*

irectional Characteristics of a U-Shaped Slot Antenna," Technical Report . 12, Richard C. Becker, 30 September 1956.**

pedance of Ferrite Loop Antennas," Technical Report No. 13, V. H. Rumsey d W. L. Weeks, 15 October 1956. AD 119780

losely Spaced Transverse Slots in Rectangular Waveguide," Technical Report . 14, Richard F. Hyneman, 20 December 1956.

Distributed Coupling to Surface Wave Antennas," Technical Report No. 15, alph Richard Hodges, Jr., 5 January 1957.

The Characteristic Impedance of the Fin Antenna of Infinite Length," Technical eport No. 16, Robert L. Carrel, 15 January 1957.*

On the Estimation of Ferrite Loop Antenna Impedance," Technical Report No. 17, alter L. Weeks, 10 April 1957.* AD 143989

A Note Concerning a Mechanical Scanning System for a Flush Mounted Line Source ntenna," Technical Report No. 18, Walter L. Weeks, 20 April 1957.

Broadband Logarithmically Periodic Antenna Structures," Technical Report No. 19, . H. DuHamel and D. E. Isbell, 1 May 1957. AD 140734

Frequency Independent Antennas," Technical Report No. 20, V. H. Rumsey, 25 ctober 1957.

The Equiangular Spiral Antenna," Technical Report No. 21, J. D. Dyson, 15 eptember 1957. AD 145019

Experimental Investigation of the Conical Spiral Antenna," Technical Report o. 22, R. L. Carrel, 25 May 1957.** AD 144021

Coupling between a Parallel Plate Waveguide and a Surface Waveguide," Technical eport No. 23, E. J. Scott, 10 August 1957.

Launching Efficiency of Wires and Slots for a Dielectric Rod Waveguide," echnical Report No. 24, J. W. Duncan and R. H. DuHamel, August 1957.

The Characteristic Impedance of an Infinite Biconical Antenna of Arbitrary ross Section," Technical Report No. 25, Robert L. Carrel, August 1957.

Cavity-Backed Slot Antennas," Technical Report No. 26, R. J. Tector, 30 ctober 1957.

Coupled Waveguide Excitation of Traveling Wave Slot Antennas," Technical eport No. 27, W. L. Weeks, 1 December 1957.

Phase Velocities in Rectangular Waveguide Partially Filled with Dielectric," echnical Report No. 28, W. L. Weeks, 20 December 1957.

Measuring the Capacitance per Unit Length of Biconical Structures of Arbitrary ross Section," Technical Report No. 29, J. D. Dyson, 10 January 1958.

Non-Planar Logarithmically Periodic Antenna Structure," Technical Report No. 30, . E. Isbell, 20 February 1958. AD 156203

Electromagnetic Fields in Rectangular Slots," Technical Report No. 31, N. J. uhn and P. E. Mast, 10 March 1958.

The Efficiency of Excitation of a Surface Wave on a Dielectric Cylinder," echnical Report No. 32, J. W. Duncan, 25 May 1958.

A Unidirectional Equiangular Spiral Antenna " Technical Report No. 33, . D. Dyson, 10 July 1958. AD 201138

Dielectric Coated Spheriodal Radiators," Technical Report No. 34, W. L. eeks, 12 September 1958. AD 204547

A Theoretical Study of the Equiangular Spiral Antenna," Technical Report o. 35, P. E. Mast, 12 September 1958. AD 204548

ontract AF33(616)-6079

Use of Coupled Waveguides in a Traveling Wave Scanning Antenna," Technical eport No. 36, R. H. MacPhie, 30 April 1959. AD 215558

On the Solution of a Class of Wiener-Hopf Integral Equations in Finite and nfinite Ranges," Technical Report No. 37, Raj Mittra, 15 May 1959.

Prolate Spheroidal Wave Functions for Electromagnetic Theory," Technical eport No. 38, W. L. Weeks, 5 June 1959.

Log Periodic Dipole Arrays," Technical Report No. 39, D. E. Isbell, 1 June 1959. D 220651

A Study of the Coma-Corrected Zoned Mirror by Diffraction Theory," Technical eport No. 40, S. Dasgupta and Y. T. Lo, 17 July 1959.

The Radiation Pattern of a Dipole on a Finite Dielectric Sheet," Technical eport No. 41, K. G. Balmain, 1 August 1959.

The Finite Range Wiener-Hopf Integral Equation and a Boundary Value Problem n a Waveguide," Technical Report No. 42, Raj Mittra, 1 October 1959.

Impedance Properties of Complementary Multiterminal Planar Structures," echnical Report No. 43, G. A. Deschamps, 11 November 1959.

On the Synthesis of Strip Sources," Technical Report No. 44, Raj Mittra, December 1959.

Numerical Analysis of the Eigenvalue Problem of Waves in Cylindrical Waveguides," echnical Report No. 45, C. H. Tang and Y. T. Lo, 11 March 1960.

New Circularly Polarized Frequency Independent Antennas with Conical Beam or nnidirectional Patterns," Technical Report No. 46, J. D. Dyson and P. E. Mayes,) June 1960. AD 241321

Logarithmically Periodic Resonant-V Arrays," Technical Report No. 47, P. E. Mayes, nd R. L. Carrel, 15 July 1960. AD 246302

Study of Chromatic Aberration of a Coma-Corrected Zoned Mirror," *Technical* port No. 48, Y. T. Lo, June 1960

valuation of Cross-Correlation Methods in the Utilization of Antenna Systems," *chnical Report No. 49*, R. H. MacPhie, 25 January 1961

ynthesis of Antenna Product Patterns Obtained from a Single Array," *Technical* *port No. 50*, R. H. MacPhie, 25 January 1961.

n the Solution of a Class of Dual Integral Equations," *Technical Report No. 51*, Mittra, 1 October 1961. AD 264557

nalysis and Design of the Log-Periodic Dipole Antenna," *Technical Report No. 52*, bert L. Carrel, 1 October 1961.* AD 264558

Study of the Non-Uniform Convergence of the Inverse of a Doubly-Infinite trix Associated with a Boundary Value Problem in a Waveguide," *Technical Report* . 53, R. Mittra, 1 October 1961. AD 264556

Copies available for a three-week loan period.

* Copies no longer available.

Antenna Laboratory

Technical Report No. 57

POLYGONAL SPIRAL ANTENNAS

by

C. H. Tang

and

O. L. McClelland

Contract AF33(657)-8460

Project No. 6278, Task No. 40572

June 1962

Sponsored by:

AERONAUTICAL SYSTEMS DIVISION

Electrical Engineering Research Laboratory
Engineering Experiment Station
University of Illinois
Urbana, Illinois